Environ Earth Sci (2013) 69:2311–2335
DOI 10.1007/s12665-012-2060-x

ORIGINAL ARTICLE

Characterization of groundwater chemistry under the influence of lithologic and anthropogenic factors along a climatic gradient in Upper Cauvery basin, South India

B. Siva Soumya · M. Sekhar · J. Riotte · Amlan Banerjee · Jean-Jacques Braun

Received: 18 April 2012 / Accepted: 15 October 2012 / Published online: 5 December 2012

Abstract Hydrogeological and climatic effect on chemical behavior of groundwater along a climatic gradient is studied along a river basin. 'Semi-arid' (500–800 mm of mean annual rainfall), 'sub-humid' (800–1,200 mm/year) and 'humid' (1,200–1,500 mm/year) are the climatic zones chosen along the granito-gneissic plains of Kabini basin in South India for the present analysis. Data on groundwater chemistry is initially checked for its quality using NICB ratio (<±5 %), EC versus TZ+ (~0.85 correlation), EC versus TDS and EC versus TH analysis. Groundwater in the three climatic zones is 'hard' to 'very hard' in terms of Ca–Mg hardness. Polluted wells are identified (>40 % of pollution) and eliminated for the characterization. Piper's diagram with mean concentrations indicates the evolution of $CaNaHCO_3$ (semi-arid) from $CaHCO_3$ (humid zone) along the climatic gradient. Carbonates dominate other anions and strong acids exceeded weak acids in the region. Mule Hole SEW, an experimental watershed in sub-humid zone, is characterized initially using hydrogeochemistry and is observed to be a replica of entire sub-humid zone (with 25 wells). Extension of the studies for the entire basin (120 wells) showed a chemical gradient along the climatic gradient with sub-humid zone bridging semi-arid and humid zones. Ca/Na molar ratio varies by more than 100 times from semi-arid to humid zones. Semi-arid zone is more silicaceous than sub-humid while humid zone is more carbonaceous (Ca/Cl ~14). Along the climatic gradient, groundwater is undersaturated (humid), saturated (sub-humid) and slightly supersaturated (semi-arid) with calcite and dolomite. Concentration–depth profiles are in support of the geological stratification i.e., ~18 m of saprolite and ~25 m of fracture rock with parent gneiss beneath. All the wells are classified into four groups based on groundwater fluctuations and further into 'deep' and 'shallow' based on the depth to groundwater. Higher the fluctuations, larger is its impact on groundwater chemistry. Actual seasonal patterns are identified using 'recharge–discharge' concept based on rainfall intensity instead of traditional monsoon–non-monsoon concept. Non-pumped wells have low Na/Cl and Ca/Cl ratios in recharge period than in discharge period (Dilution). Few other wells, which are subjected to pumping, still exhibit dilution chemistry though water level fluctuations are high due to annual recharge. Other wells which do not receive sufficient rainfall and are constantly pumped showed high concentrations in recharge period rather than in discharge period (Anti-dilution). In summary, recharge–discharge concept demarcates the pumped

B. S. Soumya · M. Sekhar
Department of Civil Engineering, Indian Institute of Science, Bangalore 560 012, India

B. S. Soumya · M. Sekhar · J. Riotte · J.-J. Braun (✉)
Indo-French Cell for Water Sciences, Department of Civil Engineering, Indian Institute of Science, Bangalore 560 012, India
e-mail: jjbraun1@gmail.com

J. Riotte · J.-J. Braun
Université de Toulouse, UPS (OMP), GET, 14, avenue Edouard Belin, 31400 Toulouse, France

J. Riotte · J.-J. Braun
CNRS, GET, 31400 Toulouse, France

J. Riotte · J.-J. Braun
IRD, GET, 31400 Toulouse, France

A. Banerjee
Centre for Earth Sciences, Indian Institute of Science, Bangalore 560012, India

A. Banerjee
Indian Statistical Institute, Kolkata 700108, India

wells from natural deep wells thus, characterizing the basin.

Keywords Groundwater · Hydrochemistry · Recharge–discharge · Silicate–carbonate weathering · Pumping

Introduction

Chemistry of rainwater naturally gets modified with atmospheric interaction and transformed during infiltration through the regolith matrix before it reaches the aquifer. Groundwater chemistry in the aquifer is further modified by water–rock interactions. Apart from this, both direct and indirect anthropogenic activities (human intervention) alter this aquifer chemistry. Recent studies (Shi et al. 2001; Broers and Van der Grift 2004; Martin et al. 2004; Ramos-Leal et al. 2007; Jalali and Khanlari 2008; Pasi and Mats 2008; Ryu et al. 2008; Fantong et al. 2009; Bharadwaj et al. 2010; Perrin et al. 2011) showed that groundwater quality of shallow/unconfined aquifer also varied along flow direction with seasonal changes due to differential evapotranspiration and precipitation. Thus, establishing the balance between geogenic, anthropogenic and climatic influences in aquifer hydrosystems is crucial due to practical aspects of developing groundwater resources for utilitarian purposes (Galuszka 2007). Main objective of this paper is to decipher the relative impacts of geogenic and anthropogenic factors on basin scale groundwater chemistry of hard rock aquifer along a climatic gradient. Hard rock aquifer system has relatively poor productivity with the available groundwater prone to pollution due to over exploitation and hence is selected for this study.

Hard rock aquifers, sometimes known as "dual permeability aquifers", are generally observed to be vertically stratified into three major layers: (i) loose regolith (saprolite and soils) porous medium, which ensures as a good storage function, (ii) underlying weathered–fissured zone, which shows a lesser degree of weathering and ensures the transmissive function of the aquifer, and (iii) deep fractured zone, wherein permeability of the unweathered rock is related to fracture network. Presence or absence of top loose regolith layer depends on combined climatic and tectonic history of the region. Quite a few regions in the hard rock aquifers have been studied to correlate mineral weathering and regional scale groundwater chemistry (Grimaud et al. 1990; Rasmussen1996; Song et al. 1999; Hidalgo and Cruiz-Sanjulian 2001; Broers and Van der Grift 2004; Bertolo et al. 2006; Rajmohan and Elango 2006; Zhu et al. 2008; Arumugam and Elangovan 2009; Fantong et al. 2009; Perrin et al. 2011).

In peninsular India, hard rock aquifers are by far the most dominant. Monsoon regime, population growth, economic development and the climatic gradient in these hard rock aquifers lead to challenging issues for the sustainable preservation of groundwater and its quality. The igneous and metamorphic rocks of South Indian Deccan plateau are subject to acute groundwater pumping for both agricultural (rural) and domestic (urban) purposes. Few studies had been carried out in these terrains to observe the impact of these direct and indirect pumping on groundwater chemistry (Maréchal et al. 2006, 2009; Rajmohan and Elango 2006; Sreedevi et al. 2006; Sukhija et al. 2006; Négrel et al. 2007, 2011; Vijith and Satheesh 2007; Ayraud et al. 2008; Arumugam and Elangovan, 2009; Reddy et al. 2009; Rao and Rao 2010; Bharadwaj and Singh 2011; Purushotham et al. 2011; Perrin et al. 2011; Rajesh et al. 2012; Sharma et al. 2012). So far some analyses have been done on sub-basin scale with the data being classified into traditional seasonal monsoon and non-monsoon periods (Song et al. 1999; Martin et al. 2004; Kumar et al. 2006; Umar et al. 2009; Purushotham et al. 2011; Rajesh et al. 2012).

The present study mainly focuses on the Kabini River basin (10,000 km^2) part of the Upper Cauvery River basin (40,000 km^2). Kabini River is the main left bank tributary of the Cauvery River (Fig. 1). Study zone sits astride the Tamil Nadu, Kerala and Karnataka states of the country. Lying on the southern part of Deccan Plateau (Peninsular India), it is developed on the Precambrian high-grade metamorphic rocks, mainly granito-gneissic, of the West Dharwar craton. Kabini basin integrates the steep climatic gradients and associated geomorphologic features of the Western Ghats rain shadow (Gunnell and Bourgeon 1997; Gunnell 1998a, b, 2000; Gunnell et al. 2003, 2007; Braun et al. 2009). At the western end of the basin, the 'humid' zone with mean annual rainfall (MAR) varying from 1,100 to 2,500 mm, is characterized by a regolith mantle composed of well-drained lateritic soils on hill slopes and hydromorphous soils in the swampy valleys overlying a deep mature saprolite ($\sim$20 m). Kaolinite is the dominant clay mineral phase in both soils and saprolite of humid zone. At the eastern end of the Kabini basin, the 'semi-arid' zone (MAR = 500–900 mm/year) is characterized by a soil cover composed of well-drained red soils (ferralsols) on hill slopes and poorly drained black soils (vertisols) in the valleys overlying a shallow immature saprolite. The clay mineral assemblage in the semi-arid zone is dominated by Ca-smectite and pedogenic carbonate accumulation is frequent in both soil types (Gunnell and Bourgeon 1997; Durand et al. 2007). The 'sub-humid' transition zone (MAR = 900–1,100 mm/year) lies in between both the end-members (humid and semi-arid zones of Fig. 1). Polyphase soil mantle characterizes this landscape with relics of lateritic soils and red–black soil system. The soil cover has recorded the past and recent climatic variations

in terms of assemblage of clays and clay minerals (e.g. Fe–Mn oxides, kaolinite/smectite) and pedogenic carbonates (Tripathi and Rajamani 2007; Violette et al. 2010).

The aim of this paper is to decipher the relative impacts of anthropogenic, geogenic and climatic factors on the groundwater chemistry along the climatic gradient. Initially the reliability of the groundwater data ($n = 120$ observation wells from 14 taluks, administrative subdivisions like a county) is checked. Secondly, threshold between pristine and polluted wells is evaluated based on the zone regolith/fractured rock interactions (shallow and deep wells). Thirdly, geogenic effect on the data below the admitted pollution level is studied. Finally, the effect of climatic gradient view through the prism of recharge–discharge processes is looked at with dilution–anti-dilution concept since the dilution of chemistry due to recharge depends on the actual rainfall reaching the water table. This concept occurring in 'recharge–discharge period' is used instead of traditional episodic 'monsoon–non-monsoon' concept to identify the periods and/or zones of actual recharge.

Field settings

Current study focuses mainly on the Kabini basin and on small adjacent regions of the Upper Cauvery basin. The study area stretches from 11° 20′ to 12° 40′ northward and from 75° 48′ to 77° 30′ eastward covering two major states, Karnataka, Kerala and Tamil Nadu of South India. This region stretches along three main climatic zones—semi-arid, sub-humid and humid, demarked in terms of annual rainfall as shown in Fig. 1. Another feature characterizing the precipitation in the study area is its irregular annual distribution i.e., unimodal and bimodal patterns, which are described below.

Climatic features

Humid zone receives highest rainfall in this study area (2,500 mm/year). Rainfall pattern in this zone is unimodal with the entire rainfall showering in single stretch (2,286 ± 874 mm/year). Entire upper Kabini basin (Fig. 1) is under humid climate experiencing a high relative

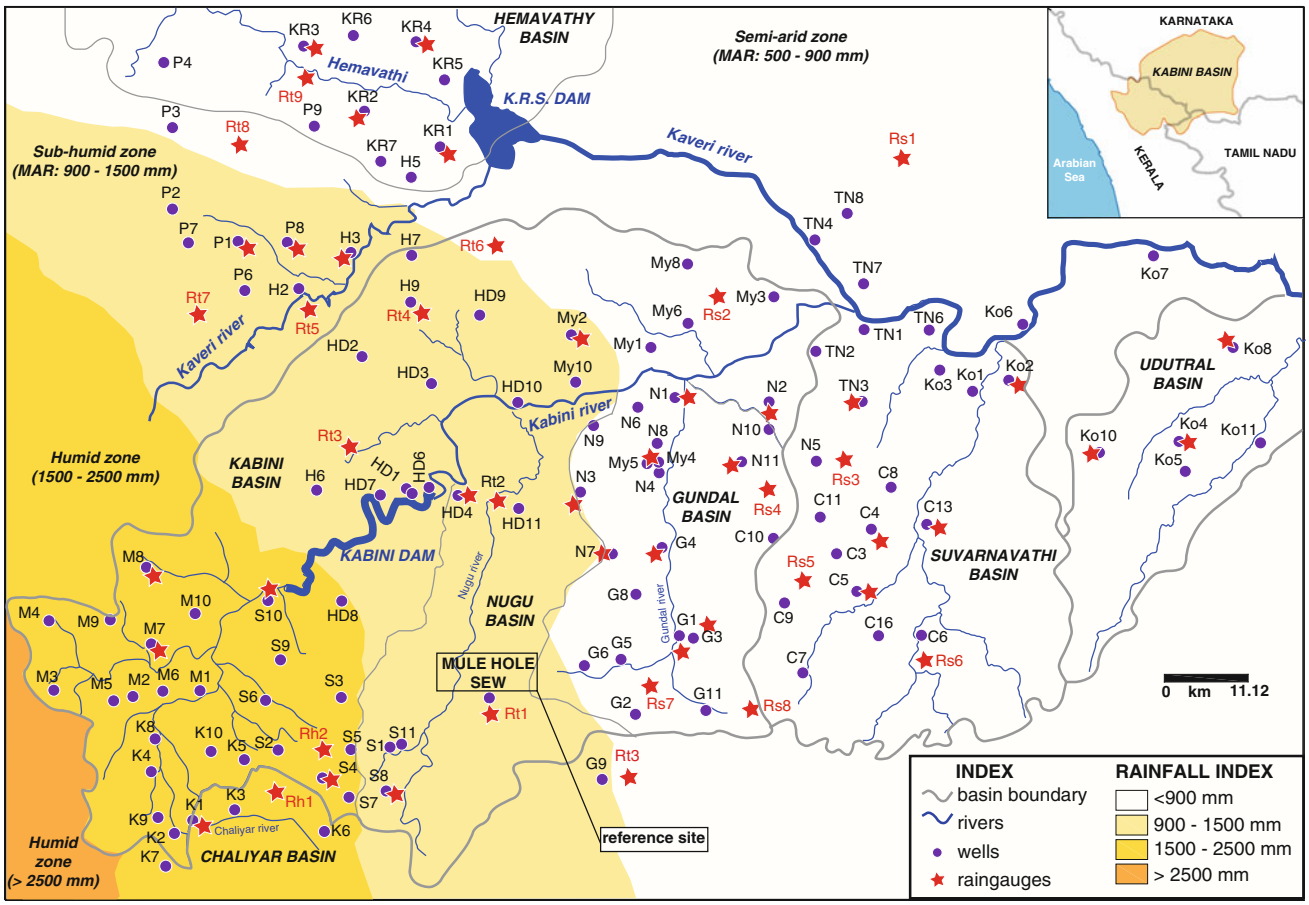

Fig. 1 Climatic gradient along Kabini River basin—study area

humidity (~95 %) during southwest monsoon. Semi–arid zone covers middle Cauvery basin and receives an annual rainfall of 730 (±250) mm. Uniqueness of this zone is the bimodal rainfall pattern with rainfall periods, once in April–May and the other during September–November of the same year. Sub-humid zone covers the entire upper Cauvery basin and a part of middle Kabini basin with an annual rainfall of 1,100 mm. Entire rainfall is distributed over 8 months (April–October or May–November) of the year. Rainfall in this zone reaches to as low as 550 mm during drought years and picks up to 1,200 mm in high rainfall years. This zone transits between humid and semi-arid zones. Temperature is lowest during December and January with mean annual temperature varying in the range of 17–37 °C, respectively.

Geological and geomorphologic features

Substratum of the study area belongs stratigraphically to the Precambrian Dharwar super group and consists of gneiss with amphibolites and quartz dykes with mean strike of N80°. A number of dykes are doleritic in composition. Most of these dykes (1.5 km length and 5–15 m wide) traverse in east–west direction (Sekhar et al. 2004). Granito-gneissic rocks cover the entire upper Cauvery basin with slight variations in the type of gneiss as shown in Fig. 2. Semi-arid and sub-humid zones are mostly covered with leucocratic gneiss while hornblende gneiss covers the humid zone (Fig. 2). Traces of ultramafics (talc–schist–pyroxene) are also found in sub-humid zone. Charnokites are predominant in eastern end of semi-arid and north-western region of sub-humid zones. These are also found in some areas of humid zone at the western end. Granites are observed to occur more frequently along the Kabini River.

Upper Cauvery basin is located in the Karnataka plateau, developed on the high-grade metamorphic silicate rocks of the West Dharwar craton. The plateau is limited westward by Western Ghats, a first-order mountain range. Due to intense periodic uplift since the Eocene, the Miocene thick lateritic mantle has almost completely disappeared and subsists at the western end of the gradient (Gunnell and Radhakrishna 2001). West–East geomorphic gradient is associated with a climatic gradient induced by the Western Ghats, which form a barrier to the north-east monsoon winds coming from Indian Ocean.

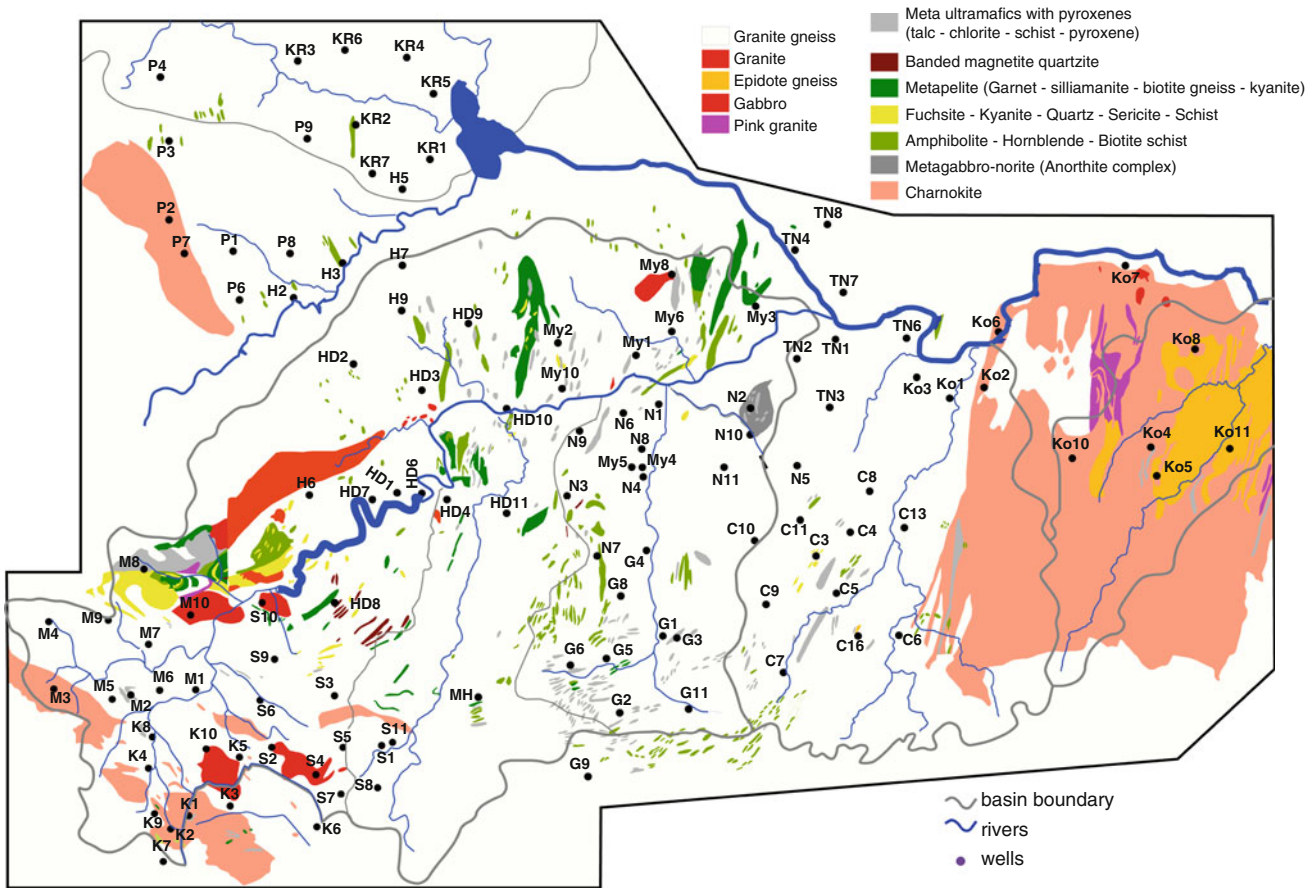

Fig. 2 Geology map of the basin

Eastward the landscape is composed of shallow regolith and outcropping inselbergs indicate that less weathered materials are now exposed. Top black soil covers contain clay minerals, Fe-oxides and oxyhydroxides. Humid zone has lateritic cover and thick mature saprolite (1:1 clay minerals with residual quartz) while semi-arid zone has shallow red soil and black soil cover (2:1 clay minerals) with thin immature regolith i.e., unweathered primary regolith (Barbiero et al. 2007). The intermediate sub-humid zone has red and black soil system with thick (20 m) immature saprolite (Braun et al. 2009).

Hydrological features

Kabini River is the main tributary to the Cauvery along with Hemavathi, Suvarnavathi and Udutral Halla (Fig. 1). The Nugu and Gundal rivers, which flow in the south–north direction (perpendicular to the climatic gradient), are the tributaries for Kabini. Nugu, Panamaram, Thirunelli, Mananthavady are the east flowing rivulets in contrast to other major west flowing rivers of the humid zone (Rajasekharan 2003). Gundal, Suvarnavathi, Udutral and Hemavathi tributaries contribute to the surface recharge in the semi-arid zone. Lineaments in this area are drainage oriented and fracture controlled, many of which are rectilinear type and trend north–south or NNE–SSW with 2.5–7.5 km length (Sekhar et al. 2004). Crisscross drainage network of perennial rivers is connected to the beneath groundwater in humid zone. Ephemeral rivers of the semi-arid zone are not connected to the baseflow. In this zone groundwater flows in the fractured rock.

Demographic and anthropogenic features

Majestic Western Ghats with lofty ridges is the prime glory of the humid zone and they are interspersed with magnificent forests. High rainfall in humid zone reduces the dependency on groundwater and hence there is almost no pumping of groundwater. Low hills are full of plantations like tea, coffee, pepper and cardamom while the valleys have predominantly paddy fields. Conjunctive usage of surface and groundwater in sub-humid zone demands pumping of groundwater sometimes. Hence, downstream areas nearer to the two major dams—Kabini dam and K.R.S dam—are prone to more pumping than rest of the sub-humid zone. Semi-arid zone is densely populated and groundwater pumping is one of the major extraction techniques. Vegetation in semi-arid and sub-humid zones is due to agricultural activity. Traditionally crops are grown during Kharif (Ragi, pulses) and Rabi season, paddy is grown in the command areas of tanks and canals. As a result of increased irrigation by bore wells, irrigated crops like sugarcane and cash crops replace traditional cropping pattern.

Small experimental watershed of Mule Hole

Mule Hole, a small experimental watershed (SEW), was set up by Indo French Cell for Water Sciences (IFCWS) in early 2000s. It is located in the sub-humid transition zone of Kabini River basin covering an area of 4.5 km^2 as shown in Fig. 1. The watershed stretches from 11° 43′N and 76° 26′E and is mostly undulating with gentle slopes and the elevation of the watershed ranges from 820–910 m above sea level. A stream passes through the center of the watershed in E–W direction. The mean yearly temperature is around 23 °C. This pristine forested watershed is covered with vegetation consisting of dry deciduous forest.

Geophysical and pedological studies in soil catena were conducted at the SEW to map the soil distribution and the erosion processes (Barbiero et al. 2007). Geophysical, mineralogical and geochemical approaches in boreholes were combined to assess the nature and the average thickness of the regolith and to study the long-term chemical mass balance (Braun et al. 2009). Hydrogeological, hydrological and geophysical approaches assessed the functioning of the groundwater reservoir (Legchenko et al. 2006; Descloitres et al. 2008), the water balance and the direct and the indirect recharge (Maréchal et al. 2009; Ruiz et al. 2010). Violette et al. (2010) attempted to model the chemical weathering processes, fluxes and the respective contribution of rock-forming and authigenic minerals at SEW. Detailed hydrogeochemical analysis of this experimental watershed, Mule Hole SEW, is explained in Soumya et al. (2011). Analysis of these experimental results is projected on to the larger Kabini basin in the following sections.

Materials and methods

A database encompassing rainfall amount, rainfall chemistry, groundwater levels and groundwater chemistry was gathered from (i) governmental agencies in both Karnataka (Department of Mines and Geology) and Kerala (Kerala Groundwater Department) and (ii) from the small experimental pristine forested watershed of Mule Hole SEW (IFCWS, Indian Institute of Science, Bangalore). Mule Hole SEW is considered as the reference threshold for the present study. Rainwater is collected for its quality analysis only when the rainfall is sufficiently large (>5 mm/day). Groundwater is sampled at different levels of the regolith mantle and in the fractured hard rock aquifer for its chemistry. Sampling details are explained in the following section.

Piezometer and rain gauge network

Semi-arid, sub-humid and humid zones are divided into several taluks as reported in Fig. 1. Kalpetta (K), Mananthavady (M), Sulthan Bathery (S) taluks of Kerala state receive heavy rainfall (humid zone). H.D. Kotte (HD) taluk sits astride in both humid and sub-humid zones of the basin. Periyapatna (P) taluk in the northern part of the basin lies in both sub-humid and semi-arid zones. Hunsur (H) is another taluk which experiences transit climate (sub-humid zone). K.R. Nagar (KR), T. Narasipur (TN), Nanjangud (N), Gundlupet (G), Chamarajanagar (C) and Kollegal (K) are the administrative taluks of this zone. Parts of Periyapatna (P) and Mysore (My) taluks also lie in this zone. Kabini River joins the Cauvery River at N1 while Suvarnavathi River meets the Cauvery River at K6 (Fig. 1).

Around ten observation wells had been set up in each of the taluks by the respective state governments for recording groundwater data. In total, around 120 sampling sites had been chosen for hydrogeochemical analysis of the groundwater as marked in the map of Fig. 1. Groundwater sampling sites are marked with a prefix denoting the taluk to which they belong suffixed by the well number. Groundwater sampling sites are shown as circles in Fig. 1 while the triangles shown in the figure are the rain gauges set up in the study area. Rain gauges are named as Rh, Rt, Rs which are located in humid, sub-humid and semi-arid zones, respectively. For some sampling points, both rain gauge and observation well are located at the same station. Rain gauge points are located in such a way that they either represent an observation well or a midpoint of 3–4 wells.

Sampling of groundwater from these wells for its chemistry, measurement of water levels in the wells and rainfall magnitude are obtained at different spatiotemporal scales. Data for 80 observation wells in Mysore and Chamarajanagar districts of semi-arid and sub-humid regions have been obtained from Department of Mines and Geology (DMG), Karnataka State (Fig. 1). Chemistry for these randomly chosen wells is from July 1993 to December 2009. 30 locations with 10 points each in the three taluks of humid zone (Upper Kabini basin) were sampled from July 1994 to December 2007 by Kerala Groundwater Department. Groundwater samples for chemistry are collected twice a year, once in pre-monsoon and later in post-monsoon period, since 1993. Both groundwater and rain water levels were measured on monthly scale using auto recorders since 1972.

In Mule Hole SEW (Gundlupet taluk), thirteen observation wells were set up at the outlet of the watershed (Soumya et al. 2011). Water samples from all these boreholes were collected twice a month from July 2003 onwards and were analyzed for the chemical parameters by IFCWS, Bangalore. Similarly, one micro-weather station was set up at Mule Hole SEW, which recorded rainfall data. Rainwater samples were collected for its chemistry on the rainy days i.e., when rainfall exceeded 5 mm/day.

Sample analysis and data selection

Experimental procedure

Samples are analyzed as per the procedures available in "Standard Methods for Water & Waste Water Analysis" (APHA 1998) for Ca^{2+}, Mg^{2+}, Na^{+}, K^{+}, Al^{3+}, F^{-}, HCO_3^{2-}, CO_3^{-}, SiO_2^{-}, SO_4^{2-}, Cl^{-} and NO_3^{2-}. Ca^{2+}, Na^{+}, Mg^{2+} and K^{+} are the dominant cations while HCO_3^{2-}, CO_3^{-}, SiO_2^{-}, SO_4^{2-} and Cl^{-} are the dominant anions. Total hardness (TH), alkalinity and physical parameters such as temperature (T), pH, electrical conductivity (EC) are also measured by the respective government departments of Kerala and Karnataka. Cations and anions are both identified using ion chromatography (IC) technique by these Kerala and Karnataka State Government Departments. Samples of Mule Hole SEW, on the other hand, were analyzed using ICP-OES for cations and ion chromatography for anions at IFCWS, Bangalore.

Selection of data for hydrogeochemical analysis

Reliability of the experimental groundwater data is checked by considering EC and molecular sum of cationic concentrations (TZ^{+}). Every water sample is checked if the difference between EC and TZ^{+} is not more than ± 10 %. EC varied from 500 to 1,500 $\mu S/cm^2$ in the semi-arid zone while it varied from 40 to 500 $\mu S/cm^2$ in the humid zone. The EC values in experimental watershed Mule Hole SEW varied in the range of 300–1,000 $\mu S/cm^2$. Sum of cationic concentration (TZ^{+}) is observed to be 10 times more than EC in magnitude i.e. varied from 4,000 to 15,000 μmol/L in semi-arid to 500–4,000 μmol/L in humid zones. In Mule Hole SEW, TZ^{+} variation is from 3,000 to 12,000 μmol/L. Hence, it is observed that EC and TZ^{+} varied linearly with a positive correlation of ~ 0.85.

Analytical precision for ions is also determined by calculating the normalized inorganic charge balance (NICB) ratio (Kumar et al. 2006) representing the fractional difference between the total cations and total anions—$\{TZ^{+} - TZ^{-}/TZ^{+} + TZ^{-}\}$. For some of the samples, carbonates (HCO_3^{-} and CO_3^{2-}) are either not measured or the measurements are erroneous (far beyond permissible limits). Further, carbonate data is sometimes obtained from measurements and sometimes from ionic balance. Hence, to obtain the best data in these cases alkalinity is estimated by setting NICB ratio as zero. Some of the samples showed

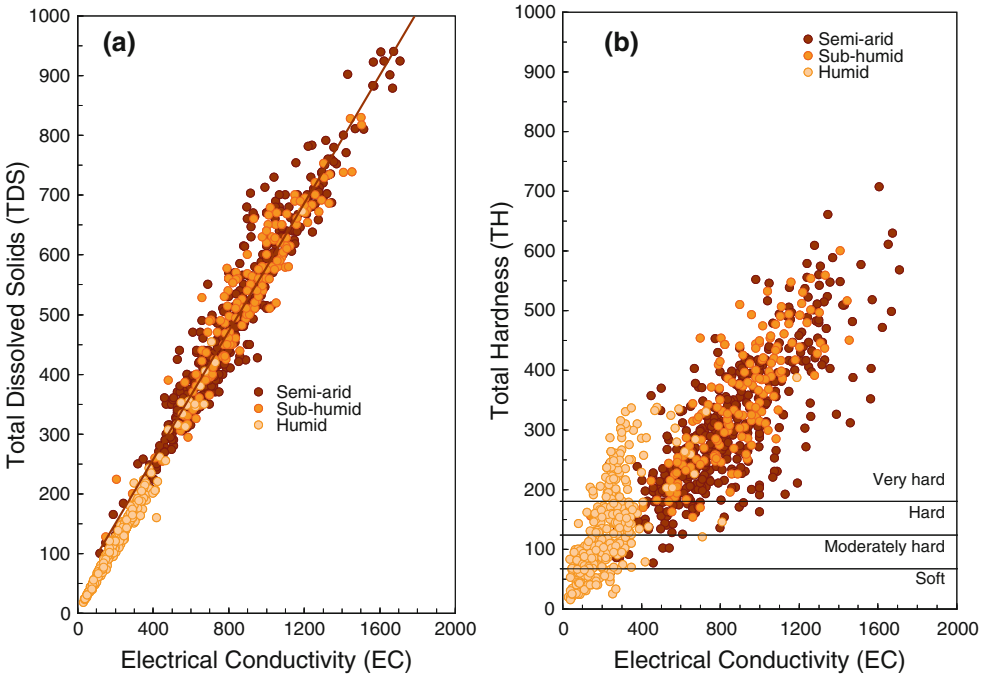

Fig. 3 Correlation between electrical conductivity and **a** total dissolved solids and **b** total hardness

a charge imbalance mainly in favor of positive excess charge, but some inversely with a negative charge deficit.

As a further check on the reliability of the groundwater chemistry data, the correlations between EC and total dissolved solids (TDS) and between EC and TH are analyzed as shown in Fig. 3. A strong linear correlation of 0.94 is observed between EC and TDS along the climatic gradient (Fig. 3a). TDS varies from 24 to 940 mg/L across the study area while EC varies from 40 to 1,670 μS/cm^2. Hence, it is observed that both EC and TDS varied 40 times along the climatic gradient, which is further supported by their strong correlation. Similarly, EC versus TH plot, shown in Fig. 3b, indicates that most the semi-arid and sub-humid zones have TH >120 mg/L (or ppm of $CaCO_3$). Groundwater in these zones varies from 'hard' to 'very hard' in terms of Ca–Mg hardness. Total hardness in the humid zone on the other hand varies from 'moderately hard' (60–120 mg/L of TH) to 'hard' (120–180 mg/L of TH) with few samples indicating 'very hard' (TH > 180 mg/L). Very few water samples in the humid zone can be said as 'soft water' with TH <60 mg/L. These high TH values might be due to the presence of dissolved carbonates, which are in nodular form in the region (Gunnell and Bourgeon 1997, Durand et al. 2007; Violette et al. 2010).

Hence, the individual water samples deviating from EC–TZ^+ linearity, EC–TDS linearity and/or having a charge balance greater than ±5 % are eliminated from the current analysis with the assumption that the data related to either EC or TZ^+ or TZ^- are subject to external influences. Apart from these criterions, which help in eliminating the erroneous data, some of the sampling stations are subject to local contamination. Such stations have to be identified and eliminated from the hydrogeochemical analysis.

Results

Effect of pollution

Water chemistry of the area, based on NICB ratio, reflects continental weathering and other anthropogenic impacts (Singh et al. 2008). Hence, influence of anthropogenic activities on groundwater is studied in terms of pollution constituency of the zone. Pollution defined as an index is used to demarcate the highly contaminated zones. Pacheco and Van der Weijden (1996) defined that pollution effect can be quantified as percentage of anion ratio (Eq. 1):

$$\%\ \text{pollution} = \frac{[Cl^-]+[SO_4^{2-}]+[NO_3^-]}{[Cl^-] + [SO_4^{2-}] + [NO_3^-] + [\text{Alkalinity}]} * 100 \quad (1)$$

where, $[\text{Alkalinity}] = [HCO_3^-] + [CO_3^{2-}]$; and all the concentrations are in μeq/L

Cl^-, CO_3^{2-} and HCO_3^- occur naturally while SO_4^{2-} and NO_3^- come from agricultural areas, all together influencing the percentage.

Percentage of pollution is calculated for every sample of each individual well and is plotted with Na/Cl as shown in Fig. 4. Moller's range of Na/Cl ratio for rainwater is shown in the figure and most of the data lie within this range. It is

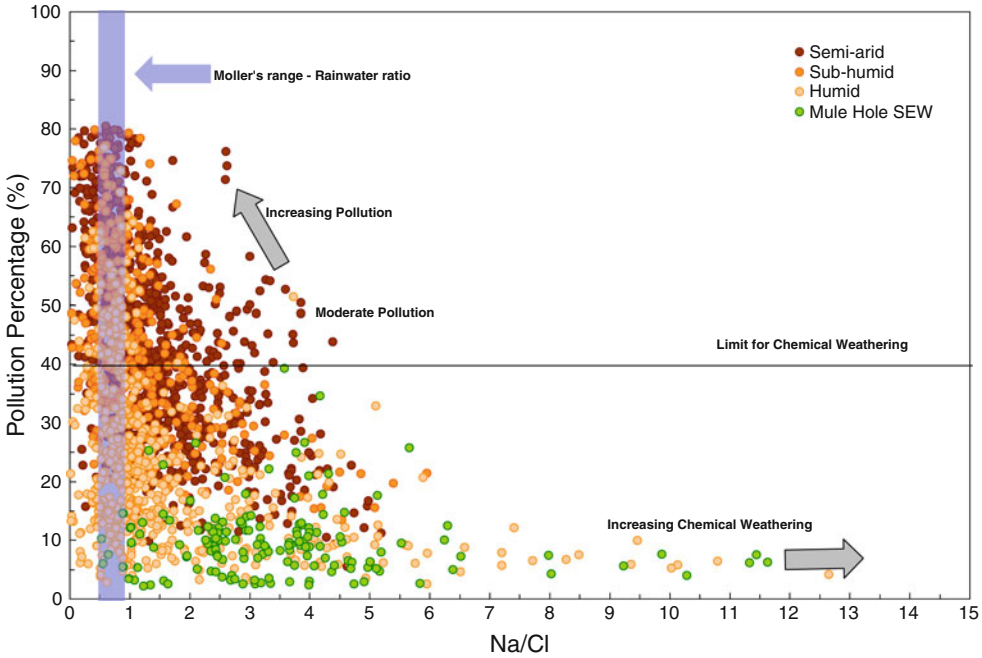

Fig. 4 Variation in pollution percentage along the climatic gradient

observed from the figure that humid zone has a wide range of Na/Cl ratios while the semi-arid zone has a narrower range. This indicates the variability in chemical weathering in the humid zone. Limit for chemical weathering is defined as 40 % in Fig. 4. Areas having ratio >40 % are dominated by pollution while those with ≤40 % are dominated by weathering reactions (Fig. 4). Water samples from both sub-humid and semi-arid zones have higher percentages of pollution indicating the increase in contamination (along *y* axis in Fig. 4). On the other hand, the small experimental forested watershed, Mule Hole SEW, has a low percentage of pollution, less than pollution limit (≤40 %). The variability in Na/Cl ratio in Mule Hole SEW indicates the extent of weathering process.

The sampling stations, which have mean anion percentage >60 % are considered to be polluted as per the definition given by Pacheco and Van der Weijden (1996). Stations whose anion percentage is in the range of 40–60 % can be considered as moderately polluted. In such stations, few sampling points sometimes result in high anion percentage ratio. This might be due to such samples showing high concentrations of Cl^-, SO_4^{2-} or NO_3^-. Such outliers are identified from Na/Cl versus Cl^- analysis at individual sample and well scale. Na/Cl versus Cl^- analysis indicates the cation exchange, a process found to occur whenever there is disturbance in the chemical equilibrium between groundwater and the exchange complex (Jalali and Khanlari 2008). Na/Cl ratio ranges from 1.0 to 3.0, implying that the geochemical evolution of groundwater is related to the mineral dissolution (Li et al. 2008). Outliers of this analysis (Na/Cl > 8 and/or Cl^- > 3,500 μmol/L) are observed to be contaminated by both Cl^- and Na^+, sources being sewage and septic tanks. With the removal of these individual samples, which are highly contaminated from the chemistry point of view, percentage of anion ratio reduced from 40–60 % to <30 %.

Mean percentages of pollution index for every well in the three climatic zones are enlisted in Table 1. Petrology of sampling sites is also presented in this table. It is observed from the table that pollution index is high in contaminated regions belonging to the three climatic zones irrespective of their geological settings. Mean percentage of pollution reduced along the climatic gradient from semi-arid (45.3 %) to sub-humid (29.8 %) to humid zones (23.6 %). Since there is variability in pollution percentage of each well, limit is set as 45 % for the semi-arid and sub-humid zones. In case of humid zone, the entire data set corresponding to a particular station has high values of Na/Cl or SO_4^{2-} or NO_3^- and such stations are marked as contaminated. All the sampling stations which have pollution percentage higher than the limit were eliminated completely from further analysis (Italic wells of Table 1). Finally, data pertaining to ideal-natural chemistry is sorted out for this characterization analysis (Roman wells of Table 1).

Descriptive statistics

At every sampling station, the mean and standard deviation of *T*, pH, EC, TH and water chemistry is calculated for the sampled data. Table 2 enlists these means and standard deviations of all the physical and chemical parameters for 'good' sampling stations (Roman wells of Table 1). Depth to groundwater is indicated in brackets as superscript

Table 1 Pollution percentage in all the wells of the three zones

Semi-arid						Sub-humid			Humid		
Well no	Geology	% pollution	Well no	Geology	% pollution	Well no	Geology	% pollution	Well no	Geology	% pollution
C3	KFQ	34.8	*My1*	*U*	*61.9*	HD1	Gg	35.8	K1	Ch	28.4
C4	*Gg*	*43.4*	*My3*	*Mp*	*44.1*	HD2	AHS	35.9	*K2*	*Ch*	*10.2*
C5	Gg	33.9	*My5*	*Gg*	*49.4*	HD4	Gg	30.6	K3	HBG	20.2
C6	*Gg*	*57.6*	*My4*	*Gg*	*57.6*	HD3	Gg	36.5	K4	HBG	12.4
C7	Gg	39.4	*My6*	*Gg*	*54.7*	HD6	Gg	30.0	*K5*	*Pg*	*29.5*
C8	Gg	34.7	My8	G	37.2	HD7	Gg	38.5	K6	HBG	29.0
C9	Gg	38.6	TN1	Gg	30.6	HD9	AHS	31.4	K7	HBG	31.6
C10	*Gg*	*49.0*	*TN2*	*Gg*	*48.6*	HD10	Gg	32.7	K8	HBG	18.1
C11	Gg	27.4	*TN3*	*Gg*	*60.0*	HD11	Gg	37.6	K9	Ch	29.3
C13	Gg	31.4	*TN4*	*Gg*	*48.5*	*H2*	*Gg*	*43.5*	K10	Pg	23.8
C16	AHS	24.5	TN6	Gg	19.8	*H3*	*AHS*	*47.5*	M1	HBG	14.3
G1	Gg	34.5	TN7	Gg	39.2	H5	Gg	29.5	M2	U	9.8
G3	AHS	31.8	*TN8*	*Gg*	*55.2*	*H6*	*Gg*	*52.7*	M3	Ch	19.8
G2	Gg	28.1	N1	Gg	38.5	H7	Gg	27.4	M4	HBG	33.0
G4	*Gg*	*48.7*	N2	U	38.5	H9	Gg	36.9	M5	HBG	30.3
G5	Gg	32.2	N3	Gg	37.9	*P1*	*Gg*	*59.2*	*M6*	*HBG*	*38.6*
G6	AHS	36.9	*N4*	*Gg*	*55.5*	*P2*	*Ch*	*48.8*	*M7*	*HBG*	*38.0*
G8	*Gg*	*55.3*	N6	Gg	29.0	*P6*	*Gg*	*66.1*	M8	U	13.6
G11	*Gg*	*47.4*	*N5*	*Gg*	*43.9*	P7	Ch	44.2	M9	HBG	26.3
Ko1	*Gg*	*52.5*	N7	AHS	38.1	*P8*	*Gg*	*57.4*	*M10*	*Gabbro*	*25.4*
Ko2	Ch	34.2	*N8*	*Gg*	*63.7*	G9	Gg	32.9	S1	HBG	14.1
Ko3	Gg	33.2	N10	Mg-n	37.6	MH	AHS	11.4	*S2*	*Pg*	*32.4*
Ko4	AHS	38.6	N9	Gg	34.2	*My2*	*U*	*54.4*	S4	Pg	20.9
Ko5	*Eg*	*47.1*	N11	Gg	37.9	*My10*	*U*	*50.5*	S3	HBG	29.0
Ko6	*Ch*	*45.5*	*P3*	*Gg*	*46.6*				*S5*	*HBG*	*45.5*
Ko7	*Ch*	*59.4*	P4	AHS	36.4				S6	HBG	27.6
Ko8	*Eg*	*48.8*	*P9*	*Gg*	*44.7*				S7	HBG	24.3
Ko10	*Ch*	*48.0*							*S9*	*HBG*	*27.9*
Ko11	*Eg*	*66.7*							*S8*	*HBG*	*45.6*
KR1	*Gg*	*47.6*							*S11*	*HBG*	*27.5*
KR2	AHS	38.0							S10	Gabbro	23.5
KR3	Gg	39.2							HD8	B	28.6
KR4	*Gg*	*53.6*									
KR5	Gg	28.9									
KR6	*Gg*	*51.9*									
KR7	Gg	36.7									

Italics indicate the pollution greater than 40 %

Gg Granite gneiss, *G* granite, *HBG* hornblende-biotite-gneiss, *Eg* epidote gneiss, *Pg* pink granite, *KFQ* kyanite-fuchsite-quartz, *AHS* amphibolite-hornblende schist, *Ch* charnokite, *U* ultramafics, *Mp* metapelite, *Mg-n* metagabbronorite, *B* banded iron formation

against the sampling station number for each of the observation wells in the first column of the table. Database collected at Mule Hole SEW is obtained from Soumya et al. (2011) and is listed for some of the wells in Table 2. Si is not determined at some of the sampling stations (semi-arid and sub-humid zones). It is observed from the table that deviation in *T* and pH are nominal. On the other hand, standard deviation in K^+ and Ca^{2+} concentrations are as high as their mean values. These high deviations might be due to the variations in vegetation patterns (agricultural effect) across the study period. SO_4^{2-} and NO_3^- are very low in the humid zone in comparison with higher values in sub-humid and semi-arid zones, which are mainly due to the fertilizer inputs in the agricultural areas.

Suitability for domestic and irrigation usage

Based on the database listed in Table 2, it is observed that many of the parameters exceed the desirable limits of WHO (1997) and BIS (1991). EC and TH in semi-arid and sub-humid zones are higher than the permissible limits of 750 μS/cm and 100 mg/L, respectively. On the other hand, ~80 % of wells in humid zone and Mule Hole SEW exhibit EC and TH within permissible limits of WHO and BIS for domestic purpose. Hardness of water is attributable to the presence of alkaline minerals primarily Ca and Mg and sometimes bicarbonates (Bharadwaj and Singh 2011; Sharma et al. 2012). Statistics show that in the study area Na^+, Ca^{2+}, Mg^{2+}, K^+, HCO_3^{2-}, Cl^-, F^- and SO_4^{2-} are below permissible limits (WHO 1997). Concentration of NO_3^- is above recommended level of 45 mg/L at some of the sampling points. Total nitrate content in groundwater might be high due to numerous sources (Purushotham et al. 2011)—atmospheric nitrogen fixation, domestic wastes and leakages from septic tanks, and fertilizers used in irrigation (urea $(NH_2)_2CO$ and ammonium nitrate NH_4NO_3).

Salinity (in terms of EC and Na %) in groundwater is a measure for its suitability for irrigation. Sodium percentage (Na %) in water samples is calculated as a percentage of $Na^+/(Ca^{2+} + Mg^{2+} + Na^+ + K^+)$ ratio. Na % varies from 8.5 to 79.6 % (average of 44 %) over the three climatic zones. As per Indian Standard (BIS 1991), maximum Na recommended for irrigation water is 60 %. The plot of analytical data on the Wilcox (1955) diagram, relating EC and Na % (Fig. 5) shows that the quality of water in the humid zone and in Mule Hole SEW is excellent to good. In contrast, 50 % of the samples in sub-humid and semi-arid zones are excellent to good with rest 50 % in good to permissible category. Few samples of semi-arid zone fall in the category of permissible to doubtful. Thus, it can be deduced from Fig. 5 that groundwater of the study area may be used for irrigation.

Hydrochemical facies

The geochemical evolution of groundwater can be understood by plotting the concentrations of major cations and anions in the Piper (1944) trilinear diagram. It is assumed that monsoon months for semi-arid, sub-humid and humid zones are August–November (including May), April–October and June–August, respectively. The filtered non-polluted database (whose statistics are described in Table 2) for Ca^{2+}, Mg^{2+}, Na^+, K^+, CO_3^{2-}, HCO_3^-, Cl^-, SO_4^{2-} and TDS concentrations is used to plot Piper's diagram as shown in Fig. 6. Database is divided among monsoon and non-monsoon months crudely irrespective of the amount of rainfall and Piper's diagram appeared to be same due to the disparities in amount of rainfall, duration of rainfall and actual recharge (explained in later sections).

In the Piper's diagram with the defined six chemical zones, it is evident that groundwater in the region had $CaHCO_3$ composition (zone 1) which evolved to mixed $CaNaHCO_3$ composition (zone 5b). This composition is more or less observed in the groundwater within the granites at most of the other regions (Tsujimura et al. 2007; Li et al. 2008; Arumugam and Elangovan 2009; Fantong et al. 2009; Bharadwaj et al. 2010). From the plot it is observed that alkaline earths $(Ca^{2+} + Mg^{2+})$ exceeds the alkalis $(Na^+ + K^+)$ and carbonates $(CO_3^{2-} + HCO_3^-)$ exceed the other anions $(Cl^- + SO_4^{2-})$. Since most of the sampling points in the diagram lie in zone 1 it can be deduced that strong acids exceed weak acids in the region.

Geochemical evaluation along the climatic gradient

The geochemical variations in the ionic concentrations of groundwater can easily be understood when they are plotted along *X*–*Y* coordinate (Guler et al. 2002). Variations in concentrations along the climatic gradient are initially studied in terms of major cations (Ca^{2+}, Mg^{2+} and Na^+). Later in this section, the trends in concentrations (both cations and anions) with depth are studied.

Sub-humid zone versus Mule Hole SEW

Chemistry at Mule Hole SEW is compared with rest of the sub-humid zone to regionalize the behavior. Chemistry of groundwater of wells in rest of the transition zone is plotted along with Mule Hole as shown in Fig. 7a. It is observed in the figure that groundwater chemistry of Mule Hole SEW is a representation of the chemistry of sub-humid zone at local scale. Mineralogy of the sub-humid zone is not sampled at a finer scale. Hence, the experiments carried out in Mule Hole (Legchenko et al. 2006; Descloitres et al. 2008; Braun et al. 2009; Maréchal et al. 2009) can be used to infer the mineralogy of the region since hydrochemistry of sub-humid zone is just a replica of Mule Hole SEW. Hence, an integrated picture of sub-humid zone chemistry in comparison to Mule Hole SEW is obtained confirming the uniformity in chemical behavior along the entire zone. Variation in Ca^{2+}, Na^+ and Mg^{2+} (Fig. 7a) arises mainly due to differences in local mineralogy. Further analysis is done by comparing the chemistry of sub-humid zone with humid and semi-arid zones, which are located on either side of this transit region. A pre-requisite for this analysis is the classification of all the wells into the above four groups as defined by Maréchal et al. (2009).

Transit from humid to semi-arid zones: regional scale

Based on the rainfall variations, it is hypothesized that the chemistry of humid and semi-arid zones would lie on either

Table 2 Statistical summary of groundwater chemistry (in μmol/L) along the three climatic zones of the study area

Station no.	Statistics	T^{++}	pH	EC^{++}	TH^{++}	Alk.*	Cl^-	SO_4^{2-}	NO_3^-	Ca^{2+}	Mg^{2+}	Na^+	K^+	Si^{2+}	F^-
Semi-arid															
$C3^{(5.5–19.0)}$	Mean	27.3	8.2	912.5	339.8	6,147.1	1,516.1	608.9	398.9	1,177	2,266	2,341.7	65.1	n.d	21.9
	SD	0.5	0.6	275.1	126.5	2,146.5	591.9	380.3	240.4	643.1	885.4	709.7	40.2	n.d	9.5
$C5^{(9.7–33.6)}$	Mean	26.9	7.8	1,172	388.2	8,341.4	2,042.1	690.2	423.4	1,574	2,309	4,125.3	247.2	n.d	12.4
	SD	0.4	0.4	454.8	157.5	3,127.3	1,295.3	557.3	143.7	712.9	955	1,532.7	148.5	n.d	4.6
$C7^{(2.3–9.2)}$	Mean	27.3	7.9	1,184.6	390.2	6,947.5	1,875.7	990.5	1,064.5	1,550	2,413	2,480.4	328.2	n.d	21.7
	SD	0.1	0.4	613.9	141.6	4,065.5	767.9	767.7	619.5	652.9	968.1	1,053.7	245.5	n.d	11.1
$C8^{(14.9–27.2)}$	Mean	26.9	7.8	867.5	313	6,059.5	1,633.4	514.8	439.9	1,551	1,584	2,585.6	76.7	n.d	22.1
	SD	0.4	0.5	231.2	71.9	1,509.9	692.2	316.5	210.7	697.9	759.5	973.9	36.2	n.d	10.4
$C9^{(2.1–7.2)}$	Mean	26.6	8.2	667.4	246.3	4,296.8	1,396.2	462.5	607.9	1,331	1,143	2,011.1	237.5	n.d	17.9
	SD	0.7	0.4	145.1	77.9	1,148.8	605.4	397.9	358.6	594.9	434.4	544.6	199.9	n.d	10.5
$C11^{(3.2–49.2)}$	Mean	26.5	8.1	787.5	250.5	5,838.6	952.9	409.7	376.3	1,249	1,320	2,953.3	334.8	n.d	23.2
	SD	1.1	0.5	237.3	97.2	1,741.4	644.1	250.3	256.6	681.7	873.5	727.3	426.2	n.d	9.8
$C13^{(4.3–32.8)}$	Mean	26.6	8.1	890.6	269.9	6,357.8	1,764.7	408.7	305.4	1,291	1,466	3,541.1	150.3	n.d	15.4
	SD	0.7	0.6	249.6	116.9	2,340.2	779.9	341.3	265.7	959.7	762.7	1,290.1	120.3	n.d	8.2
$C16^{(4.5–25.4)}$	Mean	26.3	7.9	700.1	268	5,748.9	1,020.1	173.8	379.1	1,443	1,331	1,791.4	140.6	n.d	20.3
	SD	1	0.6	237.6	96.8	1,771.7	550.5	154.2	250.1	625.2	571.4	725.6	94.7	n.d	10.7
$G1^{(18.3–42.6)}$	Mean	26.8	8.1	1,176.3	331.3	8,083.1	2,270.6	649.9	569.9	1,108.5	1,904.8	6,192.7	232	n.d	34.7
	SD	0.3	0.8	273.5	148.1	2,681.4	448.3	449.2	428.8	838.5	639.5	2,390.4	185.1	n.d	17.8
$G2^{(4.1–10.2)}$	Mean	26.3	8.2	1,056.4	349.6	8,072	2,061.2	449.1	422	1,239.8	2,481.8	3,785.9	228.2	n.d	37.7
	SD	0.9	0.4	277.3	121.8	3,301.3	842.7	264.1	315.9	586.6	1,733.2	1,516.6	211.5	n.d	22.7
$G3^{(5.2–44.6)}$	Mean	25.9	7.9	845.9	336.8	6,023.3	1,012.9	326.2	861.3	1,393	2,122.8	1,927.7	172	n.d	11.5
	SD	0.2	0.5	420.9	153.9	1,662.7	677.8	224.1	804.8	1,023	851.3	899.6	161.8	n.d	4.1
$G5^{(2.1–10.1)}$	Mean	25.4	8.3	687	282.5	5,347.7	1,513.7	387.3	372.6	1,016.7	1,755.8	1,863.9	496.1	n.d	15.5
	SD	0.3	0.4	292.8	135.9	2,148.9	755.1	260.3	340.4	893.2	609.9	833.9	329.5	n.d	11.4
$G6^{(2.1–9.0)}$	Mean	25.8	8.2	811.8	323.7	5,564.8	1,537.2	513.2	715.9	1,295.9	1,888.2	2,211.6	286.8	n.d	22.1
	SD	0.7	0.5	202.3	120.8	1,554.7	533.1	400.3	386.6	883.1	602.2	681.7	225.3	n.d	12.4
$Ko2^{(9.1–17.2)}$	Mean	27.6	8.1	749.2	287.4	5,417.6	1,559.5	423.2	550.4	1,693	1,402	1,969.4	163.5	n.d	5.14
	SD	0.8	0.6	218.6	108.7	2,007.4	855.1	345.1	370.5	894.3	590.1	872.7	140.1	n.d	0.2
$Ko3^{(4.7–14.5)}$	Mean	27.5	7.9	1,097.6	474.4	7,531.2	1,814.1	417.8	1,025.2	1,626.8	2,751.7	2,373.1	159.2	n.d	36.9
	SD	0.8	0.5	249.7	199.2	2,155.8	615.1	177.8	601.8	637.2	1,160.6	1,015.8	138.2	n.d	15.9
$Ko4^{(10.9–15.2)}$	Mean	27.1	8.1	1,175.2	414	6,427.3	1,700.4	512.7	991.1	1,461	2,689	3,694.1	42.6	n.d	22.9
	SD	0.6	0.3	599.9	210.7	3,185.8	691.1	270.8	803.9	663.7	1,411	1,801.2	29.5	n.d	12.5
$KR2^{(2.7–4.8)}$	Mean	26.2	8.1	796.2	284.8	5,537.1	1,643.4	570.7	407.7	1,321.1	1,479.3	2,947.6	90.5	n.d	30.3
	SD	0.8	0.5	271.7	94.5	1,632.1	661.2	335.1	301.5	672.9	493.2	1,508.3	75.7	n.d	17.9
$KR3^{(9.2–13.5)}$	Mean	26.3	8.2	826.6	286.4	4,843.1	1,955.6	366.7	738.4	1,275	1,472	2,702.8	92.7	n.d	15
	SD	1.1	0.4	187.7	65.7	1,315.1	665.3	245.1	385.2	425.1	536.5	903.5	52.8	n.d	10.2
$KR5^{(6.0–13.5)}$	Mean	26.9	8.1	661	245.9	5,385.5	1,039.2	273.9	327.8	1,030	1,486	2,052.2	219.9	n.d	16.9
	SD	0.8	0.6	157.5	71.6	2,133.6	398.3	177.4	275.2	572.9	721.7	840.5	191.1	n.d	11.7
$KR7^{(3.1–7.3)}$	Mean	26.9	7.9	827.8	292.2	5,612.6	1,662.1	470.2	631.5	1,090.2	1,870.8	2,607.7	294.1	n.d	29.1
	SD	0.6	0.9	265.6	81.5	2,049.1	615.3	296.8	315.3	550.1	609.8	1,031.4	272.5	n.d	16.9
$My8^{(16.7–26.6)}$	Mean	27.3	8.1	818.5	338.8	5,613.1	2,331.2	383.5	578.7	1,850	1,484	2,380.9	79.6	n.d	15.5
	SD	0.8	0.6	335.7	153.3	2,390.3	1,087.2	253.4	493.8	1,415	841.7	1,312.1	41.3	n.d	8.9
$P4^{(0.8–10.1)}$	Mean	26.5	7.9	687.3	274.8	5,002.8	1,356.3	292.4	787.1	1,131.1	1,745.5	1,855.4	42.6	n.d	10.9
	SD	0.8	0.6	334.5	156.7	2,495.8	832.3	270.3	668.9	550.6	1,127.2	1,117.5	26.4	n.d	5.1
$TN1^{(4.6–12.2)}$	Mean	27.9	8.1	857.6	325.1	6,374.2	1,374.6	396.3	511.5	1,335	2,038.4	2,363.5	56.8	n.d	44.8
	SD	0.9	0.6	270.8	97.1	2,511.1	607.2	274.5	266.6	799.8	491.6	896.6	50.8	n.d	11.8
$TN6^{(0.9–4.8)}$	Mean	26.7	8.2	791.8	241	5,422.3	850.2	304.1	241.9	1,071	1,355.1	2,379.9	127.8	n.d	16.1
	SD	0.5	0.4	281.4	95.1	1,844.9	699.4	189.2	220.8	570.3	487.3	985.7	86.5	n.d	10.4
$TN7^{(4.5–11.6)}$	Mean	26.1	7.9	563.3	174.8	3,418.9	1,368	210.8	540.3	989.7	857.4	1,856.7	468.9	n.d	39.6
	SD	0.6	0.7	244.1	89.5	1,636.4	890.6	189.7	276.9	705.9	709.5	800.3	257.1	n.d	23.8
$N1^{(2.3–4.7)}$	Mean	26.8	8.1	1,270.6	359.9	7,572.5	3,134	813	844.1	1,629.2	2,032.9	5,335.1	190	n.d	14.2
	SD	0.8	0.7	430.9	135.7	4,398.5	837.2	473.1	535.1	1,170.2	1,173.9	2,341.2	278.2	n.d	5.4

Table 2 continued

Station no.	Statistics	T^{++}	pH	EC^{++}	TH^{++}	Alk.*	Cl^-	SO_4^{2-}	NO_3^-	Ca^{2+}	Mg^{2+}	Na^+	K^+	Si^{2+}	F^-
N2$^{(0.8–8.0)}$	Mean	26.8	8.1	796.9	252.7	4,416.9	1,812.7	386.6	709.7	1,498.7	1,059	2,274.4	413.4	n.d	17.3
	SD	0.9	0.4	347.2	87.2	2,331.6	981.8	225.6	437.9	625.4	468.1	1,923.9	320.1	n.d	12.3
N3$^{(4.0–9.8)}$	Mean	26.8	8	869.1	325.1	5,673.4	2,240.8	663.3	548.4	1,086.7	2,222.2	2,707.7	207.8	n.d	20.4
	SD	0.6	0.5	362.9	176.3	3,259.6	983.3	338.2	431.4	569.4	1,454.4	2,162.4	188.2	n.d	19.5
N6$^{(2.1–6.0)}$	Mean	27.5	8.2	819.2	317.5	5,741.5	1,392.7	412.2	460.2	1,330.2	1,895.6	1,550.3	442.6	n.d	22.7
	SD	0.5	0.4	215.2	89.2	1,232.4	644.4	176.4	233.8	540.3	514.5	482.9	331.1	n.d	9.9
N7$^{(5.7–11.7)}$	Mean	26	8	1,021.8	385.7	6,693.6	2,049.7	747.4	642.5	1,478.9	2,420.5	2,832.5	196.1	n.d	22
	SD	0.4	0.4	311.7	122.9	2,422.2	738.6	393.8	366.4	798.2	861.1	1,235.1	163.3	n.d	12.4
N9$^{(7.3–12.0)}$	Mean	27.2	8	728.9	340.2	5,490.4	1,461.8	288.7	449.5	1,803.7	1,510.5	1,059.7	163.7	n.d	14.3
	SD	0.5	0.5	292.1	149.7	2,585.3	696.5	199.2	185.9	1,139.6	908.6	442.2	132.8	n.d	8.1
N10$^{(8.3–20.2)}$	Mean	27.5	7.9	1,113.7	381.9	7,384.8	2,401.6	505.8	741.9	1,502.8	2,136.8	3,919.8	283.4	n.d	11.6
	SD	0.7	0.6	309.5	133.4	2,613.5	554.1	178.4	300.5	913.8	716.8	1,215.7	99.6	n.d	5.3
N11$^{(15.2–23.2)}$	Mean	27.2	8.1	1,250.2	401.7	9,025.4	2,204.8	615.8	923.1	1,535.4	2,475.5	4,840.3	377.7	n.d	35.4
	SD	0.5	0.6	481.1	154.3	4,268.8	692.8	411.6	497.8	1,084.2	757.7	2,322.9	155.9	n.d	18.6
Sub-humid															
G9$^{(2.6–9.4)}$	Mean	25.7	7.9	887.4	309.3	6,169	2,052	410.9	169.4	1,721.6	1,311.7	2,521.2	641.1	n.d	40.9
	SD	0.2	0.6	215.5	83.6	1,749.5	697.5	184.8	112.1	980	776.6	850.7	540.6	n.d	18.8
HD1$^{(4.5–11)}$	Mean	25.7	8.1	1,007.9	408.9	7,281	2,609.1	303.6	591.8	1,549.2	2,375.6	2,781.1	159.1	n.d	15.9
	SD	1.4	0.5	255.2	112.8	2,556.3	776.4	177.7	380.2	970.5	894.1	618.1	80.7	n.d	11.7
HD2$^{(10.8–25)}$	Mean	26.3	8.2	965.5	344.5	6,896.9	1,651	516	679.7	1,307.8	1,989	3,089.6	135.5	n.d	31
	SD	0.6	0.5	278.2	108.2	2,594.4	704.3	167.6	445.5	707.6	714.2	1,041.6	120.6	n.d	15.6
HD3$^{(11–22.4)}$	Mean	25.9	7.9	1,018.4	485	6,506.6	1,730	284	1,077.4	1,805.3	2,410.3	2,042.1	122.8	n.d	24
	SD	0.3	0.4	210.4	130.9	3,180.4	674.2	174.5	544.9	761.2	765.9	964.1	93.2	n.d	17.5
HD4$^{(11–15.4)}$	Mean	26.6	7.9	794.6	346.9	3,855.1	1,901.1	222.1	572.6	1,411.1	1,296.3	892.1	42.6	n.d	20.6
	SD	1.8	0.5	533.8	245.6	2,319.4	1,109.9	52.9	460.4	892.7	859.6	443.8	13.2	n.d	13.5
HD6$^{(6.4–29.2)}$	Mean	26.1	8	923.7	364.4	6,896.3	1,581.2	304.5	423.7	1,344.2	2,183.6	2,638.2	136.4	n.d	16.4
	SD	1.1	0.5	310.8	121.9	2,196.1	827.8	177.8	293.9	676.6	1,060.8	1,160.3	80.7	n.d	7.7
HD7$^{(18.9–27.7)}$	Mean	27	8	938.7	396.4	6,074.3	2,096.7	551.7	621.9	1,968.1	1,939	1,748.3	235.3	n.d	16.7
	SD	0.6	0.5	312.3	134.8	1,765.9	746.5	335.3	328.1	762.5	917.6	816.3	73.1	n.d	8.2
HD9$^{(4.4–10.5)}$	Mean	26.1	8.1	824.8	334	6,494.2	1,305	517	496.8	1,447.1	2,030.2	2,312.2	153.4	n.d	21
	SD	0.7	0.5	256.8	113.8	2,525.9	580.6	377.1	280.3	746.3	588.1	1,134.1	86.1	n.d	9.7
HD10$^{(2–7)}$	Mean	25.6	8.3	1,383.3	465.3	9,957.6	2,188	861.4	737.3	904.4	3,419.1	5,850.9	364.4	n.d	38.5
	SD	0.7	0.6	461.4	164.1	4,023.6	1,030.8	743.5	329.8	536.6	1,303.3	2,694.2	426.1	n.d	29.7
HD11$^{(9.5–11.8)}$	Mean	25.8	8.1	864.2	327.8	4,637.4	1,852.2	734.7	720.4	1,322.4	1,984.5	1,445.7	204.6	n.d	btl
	SD	0.8	0.4	276.5	108.8	1,262.5	1,364.2	627.3	519.9	913.3	513.1	673.8	102.3	n.d	btl
H5$^{(6.7–9)}$	Mean	26.3	8.2	1,073.7	378.3	7,923.5	1,705.7	402.5	783.5	796.6	2,677.6	4,200.8	134.3	n.d	41.4
	SD	1.2	0.6	199.7	101.2	1,752.6	528.6	244.2	357.5	507.6	774.5	977.5	75.7	n.d	20.9
H7$^{(9.9–15.5)}$	Mean	26.4	8	1,231.4	490.5	10,905.3	1,436.8	468.8	1,273.9	1,740	3,734.2	3,480.4	232.2	n.d	9.3
	SD	1.4	0.4	279.6	103.7	2,258.8	871.5	311.6	715.7	707.7	1,044.8	1,533.2	164.5	n.d	7.6
H9$^{(6–15.1)}$	Mean	26.1	8	864.6	371.1	5,678.9	2,311.3	527.7	578.6	1,359.8	2,412.6	1,937.9	86.6	n.d	15.7
	SD	0.9	0.5	241.2	120.5	1,465.8	991.6	310.1	250.7	592.3	674.1	666.5	60.5	n.d	6.9
P7$^{(1.9–11.1)}$	Mean	26.2	8	762.8	294.3	4,871.7	2,104.2	214.3	739.8	1,467.1	1,519.9	1,943.7	113	n.d	18.7
	SD	0.6	0.4	128.2	91.1	1,646.2	569.2	150.8	418.4	690.9	837.7	867.9	66.7	n.d	13.5
Humid															
K1$^{(3.4–5.4)}$	Mean	n.d	7.3	219.6	67.2	2,099.2	694.7	37.1	123.1	754.4	314.7	778.9	77.1	743	14.4
	SD	n.d	0.6	50.1	27.6	1,032	222	47	39.5	415.3	223.7	391.2	32.4	349.6	9.7
K3$^{(2.6–11.1)}$	Mean	n.d	7.9	348.9	97.2	3,048.3	474.6	48	80.9	1,170	424.7	539.2	131.3	1,373.6	16.1
	SD	n.d	0.6	453.1	20.7	1,352	88.1	32.9	53.6	487.8	174.9	232	55.8	67.1.5	12.7
K4$^{(3.6–5.4)}$	Mean	n.d	8.3	339.3	132.5	5,178	251.7	158.9	18.7	1,576	583	909.5	214.3	1,151.2	23.8
	SD	n.d	0.4	99.8	30.8	2,547.5	83.2	85.6	15.9	963.5	198.1	275.1	118	153.2	16.9
K6$^{(7.5–10.1)}$	Mean	n.d	7	242.8	67.5	2,623.1	774.9	20.8	162.4	1,055.3	275.4	703	129.6	367.9	8.6
	SD	n.d	0.9	48.1	20.9	2,159.5	205.6	12.1	68.2	1,083.7	135.2	261.3	52.9	104.8	5.1

Table 2 continued

Station no.	Statistics	T^{++}	pH	EC^{++}	TH^{++}	Alk.*	Cl^-	SO_4^{2-}	NO_3^-	Ca^{2+}	Mg^{2+}	Na^+	K^+	Si^{2+}	F^-
$K7^{(0.3–2.3)}$	Mean	n.d	7.4	77.8	32.4	939.1	267.2	37.8	37.1	436.7	160.7	170.6	15.7	324.4	14.2
	SD	n.d	0.6	19.5	9.2	485.3	96.2	20.3	20.2	252.2	136.6	78.1	6.3	89.8	3.8
$K8^{(6.5–8.3)}$	Mean	n.d	7.4	99.8	43.4	1,436.3	234	24	20.2	620.7	155.2	166.6	21.9	586.2	6.4
	SD	n.d	0.5	47.1	16.1	889.9	123.1	38.1	22.6	386.3	112.1	66.4	10.5	230.2	1.4
$K9^{(5.4–7.4)}$	Mean	n.d	7.4	185.9	65.4	1,747.2	465.9	80.1	83.2	769	186.4	364.9	174.8	460.6	13.8
	SD	n.d	0.6	113.9	42.5	1,340.1	149.3	79.5	49.5	622.4	119.3	185.3	91.9	92.4	6.9
$K10^{(1.2–2.5)}$	Mean	n.d	7.5	247.1	82.8	2,480.7	553.2	126.2	8.3	951.9	333.9	484	67.6	738.8	5.8
	SD	n.d	1.3	106.9	35.8	1,797.3	111.8	78.8	6.8	724.3	193.7	349.6	53.8	330.6	0.7
$M1^{(2–13)}$	Mean	n.d	8	200.7	78.5	2,692.3	279.7	43.5	17.1	880.5	390.3	480.6	52.7	1,614.6	17.6
	SD	n.d	0.5	72.9	25.6	1,224.1	98.5	30.6	10.8	557.6	216.9	226.9	44.1	511.4	12.4
$M2^{(10.5–17.5)}$	Mean	n.d	8	306.4	134.8	3,709.6	324.4	33.6	24.2	1,460.8	505.3	242.5	166.9	1,081.5	14.9
	SD	n.d	0.6	107.7	34.5	1,939.9	142.1	26.6	27.4	808.4	285.9	159.1	122.7	861.1	12.5
$M3^{(2.2–7)}$	Mean	n.d	7.6	127.3	57.5	1,887	283.4	46.5	14.4	761.4	218	284.3	81.8	751	12.5
	SD	n.d	0.7	70.9	34.9	1,414.2	133.9	35.2	11.9	627.4	166	211.1	61.3	471.1	11.1
$M4^{(5.6–7.9)}$	Mean	n.d	7.7	187.8	63.3	1,916.8	369.4	81.3	14.6	771.2	205.2	439.3	65.2	748.4	27.4
	SD	n.d	0.6	63.7	27.8	1,527.6	213.9	88.1	12.2	486.1	100.3	265.8	51.8	417.7	17.3
$M5^{(8.2–13.1)}$	Mean	n.d	8	276	118.1	4,303.8	220.7	42.4	14.2	1,632.9	406.6	450.1	159.3	1,252.7	19.1
	SD	n.d	0.6	87.1	36.4	2,132.1	81.8	23.3	10.6	990.4	182.8	295.8	111.3	462.3	12.7
$M8^{(1.8–9.7)}$	Mean	n.d	7.4	76.8	35.6	1,111.2	211.2	19	12.6	464.2	140.5	161.3	20.2	340.8	10.5
	SD	n.d	0.6	44.1	14.4	635.2	101.4	10.3	10.1	314.8	129.7	47.9	11.3	149.5	6.3
$M9^{(0.7–2.0)}$	Mean	n.d	7.5	81.7	32.8	852.2	290.7	12.9	25	406.5	97.4	218.7	43.5	311.2	23.9
	SD	n.d	0.7	29.1	10.2	692.1	86.3	4.5	5.6	328.1	55.8	166.7	41.2	248.1	11.9
$S1^{(2.1–10.6)}$	Mean	n.d	8	213.4	77	2,467.2	414.4	47.6	3.8	996.3	266.9	523.2	80.9	679	7.9
	SD	n.d	0.6	101.3	38.1	1,465.3	303.1	33.4	3.1	583.5	192.2	349.1	75.5	228.1	3.9
$S3^{(5.9–17.6)}$	Mean	n.d	7.8	269.7	102.4	2,879.8	451.3	64.9	61.5	979.7	519.7	545.3	46.3	994.7	16.2
	SD	n.d	0.6	75.9	30.2	1,333.3	214.6	49.3	49.4	546.1	232.3	294.3	23.9	456.6	12.1
$S4^{(3.5–4.8)}$	Mean	n.d	7.5	200.4	46.6	1,580.9	546.8	22.5	122.3	682	150	601	89.5	740.6	10.9
	SD	n.d	0.6	83.2	12.4	954.9	131.9	19.3	40.2	457.5	68.6	207.4	44.2	257.3	6.2
$S6^{(0.1–1.3)}$	Mean	n.d	7.8	350.2	97	2,967.3	756.4	77.1	99.4	1,197	375.7	875.5	50	1,160.7	13.9
	SD	n.d	0.5	145.5	33.9	1,517.8	101.6	46	43.8	790.8	149.6	284.7	23.9	253.7	10.6
$S7^{(5.5–9.5)}$	Mean	n.d	7.4	160.8	47.5	1,746.5	356.4	28.4	27	711.2	71.3	263.9	243.9	654	10.5
	SD	n.d	0.7	61.7	40.6	1,259.3	89.2	21.5	10.6	590.8	32.9	118.7	189.4	197.6	6.6
$S10^{(4–8.9)}$	Mean	n.d	8.2	405.3	121.6	3,279.8	749.5	140.5	88.5	1,256.5	537	774	56.6	1,121.6	20.6
	SD	n.d	0.5	214.1	48.2	2,484.1	146.4	63.2	63.9	966.4	234.5	325.6	39.8	506.7	18.8
$HD8^{(4.2–15.1)}$	Mean	26.1	7.9	656.4	282.3	4,823.7	1,316.3	204.7	479.8	1,143.9	1,396	1,660.9	62.1	n.d	16.2
	SD	0.8	0.5	347.4	114.9	2,613.8	711.3	191.4	271.6	630.3	684.4	1,488.9	35.7	n.d	8.9
Mule Hole SEW															
$MH2^{(18.9 - 23)}$	Mean	25.6	7.4	480.7	189.5	4,280	174.1	28.8	10	1,453.9	459.7	510.1	226.8	409.6	6
	SD	0.72	0.6	169.8	51.2	1,270.2	144.2	36.7	8.1	412.3	427.2	476.4	104.8	165.6	2.4
$MH3^{(27.6–28.9)}$	Mean	25.7	7.6	586	203.4	4,951	401.6	88.5	18.1	1,330	960.1	1,425.3	251.1	858.6	9
	SD	0.7	0.6	184.5	76.2	1,816.7	203.1	83.4	13.3	452.5	441.3	113.5	77.9	198.9	6.6
$MH5^{(39.8–40.8)}$	Mean	25.3	7.2	660.9	255.8	6,041.9	511.2	34.7	21.3	1,596.2	1,096.1	1,331.8	211.7	786.2	8.8
	SD	1.2	0.5	38.7	43.8	854.8	64.8	13.7	16.9	245.1	99.4	133.7	51.1	115.6	4.3
$MH6^{(37.7–38.5)}$	Mean	25.1	7.2	917.5	408.5	8,635.3	257.3	202.4	17.7	2,529.1	1,767.9	1,013.2	143.5	627.2	4.3
	SD	0.9	0.5	73.3	74.9	1,500.8	87.4	54.4	12.9	412.1	169.5	183.3	51.8	79	0.9
$MH8^{(8.1–12.8)}$	Mean	24.9	7.1	675.7	181.4	4,382.9	281.2	275	12.1	2,062.3	1,019.8	1,181.9	103.8	837.1	10
	SD	0.9	0.7	142.8	79.5	1,550.3	213.1	138.4	4.8	1,385.7	268.8	310.5	53.2	122.7	3.9
$MH13^{(9.1–12.5)}$	Mean	25.2	7.3	364.2	85.1	2,206.9	92.8	14.9	3.1	351.8	499.9	570.3	56.2	720.6	7.2
	SD	1.6	0.7	15.3	15.1	409.2	33	12.7	2.4	53.6	106.5	141.3	14.3	53.5	1.3

The values in the parenthesis indicate the range of depth to groundwater

n.d Not determined, *btl* below detection limit

* Alkalinity is computed from NICB ratio

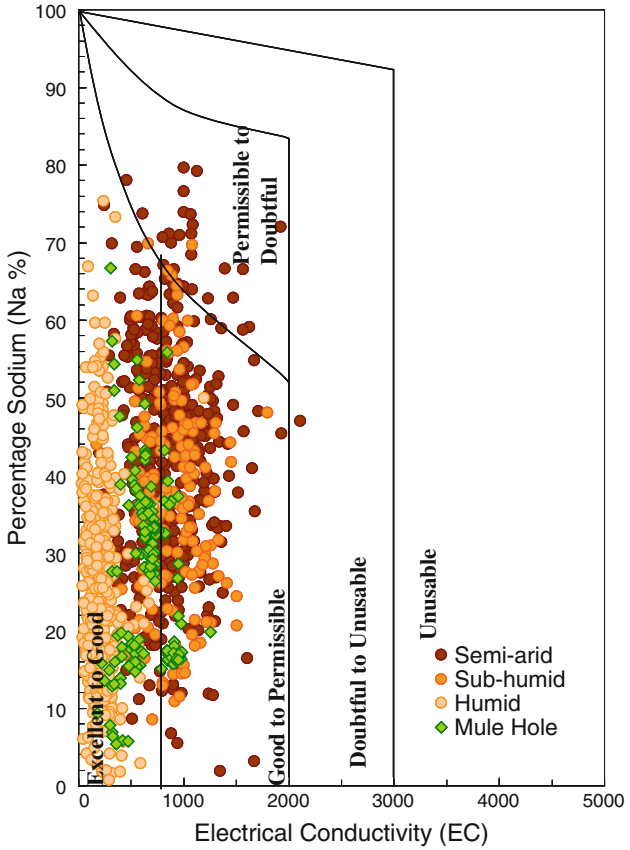

Fig. 5 Wilcox diagram—EC versus Na %

end of the sub-humid zone. To confirm this hypothesis, the plot of Fig. 7a is extended for the entire basin showing the chemical gradient along the climatic gradient, as shown in Fig. 7b. This extension to regional scale shows that chemistry follows gradient in response to the gradient in rainfall. Sub-humid zone mainly consists of gneiss with few locations containing feldspar (Braun et al. 2009). In terms of chemistry of groundwater in the basin, humid zone clusters near the 'carbonate' end-member (Fig. 7b) while semi-arid zone clusters near the 'silicate' end-member (Ryu et al. 2008) due to the presence of high Ca^{2+} in humid (hornblende gneiss, Fig. 2) and due to high Na^{+} in semi-arid zones (leucocratic gneiss). Sub-humid zone bridges between semi-arid and humid zones with a clear shift from one zone to another. Scatter in terms of Mg/Na ratio is due to water–rock interactions resulting from frequent small showers.

Saturation indices

Saturation index of a given mineral is calculated using the formula

$$SI = \log_{10}\left(IAP_i/K_{spi}\right) \quad (2)$$

where IAP_i is ion activity product of species i in the solution and K_{spi} is the solubility product of the species i at a given temperature. If $SI_i > 0$, then precipitation of the species i is thermodynamically possible; whereas $SI_i < 0$ means the species i will favor dissolution. The default "PHREEQC for Windows" database and PHREEQC software is used for the saturation index calculations. These indices of calcite and dolomite in the groundwater are shown in Fig. 8.

Figure 8a, b shows the plots of obtained SI against EC ($\mu S/cm^2$) for calcite and dolomite, respectively. It is observed from the plot that for most of the samples in humid zone, $SI_{Calcite}$ and $SI_{Dolomite}$ both are <0, while both the indices are >0 in sub-humid and semi-arid regions. Thus, groundwater is mostly undersaturated with respect to calcite and dolomite in the upstream humid climatic condition, while it become saturated and slightly oversaturated with respect to calcite and dolomite downstream along sub-humid to semi-arid climatic conditions.

Controlling mechanisms

Gibbs's diagrams representing the ratios of $[Na^+/(Na^+ + Ca^{2+})]$ and $[Cl^-/(Cl^- + HCO_3^-)]$ as a function of TDS, are widely employed to assess the functional source of dissolved chemical constituents, such as precipitation dominance, rock dominance and evaporation dominance (Gibbs 1970). Ratios of cations and anions (Gibbs plot) are plotted against TDS for all the three climatic zones as shown in Fig. 9. Chemical data for both semi-arid and sub-humid zones cluster around the zone of rock domain. On the other hand, ionic ratios spread from the zone of precipitation toward rock domain in humid zone, indicating the control of precipitation on water quality. Low TDS values observed in humid zone correspond to the monsoon period. Thus, mechanism controlling groundwater chemistry at Upper Cauvery Basin shows that the quality is originally regulated by geogenic process and subsequently influenced by precipitation during monsoon period especially when rainfall is sufficient enough to recharge the aquifer below.

Mineralogical interactions

Shift in the geochemical behavior along the climatic zones (Fig. 7b) indicates the prominence of input from rainfall and weathering. Low $Cl/\sum_{anions}$ (median = 0.2) supports that Cl is derived mainly from atmospheric sources and would be present in groundwater as NaCl (Kortatsi et al. 2008). In order to identify the major mineralogical reactions dominating the zones, Na^+ versus Cl^- and $(Ca^{2+} + Mg^{2+})$ versus Cl^- plots are used (Soumya et al.

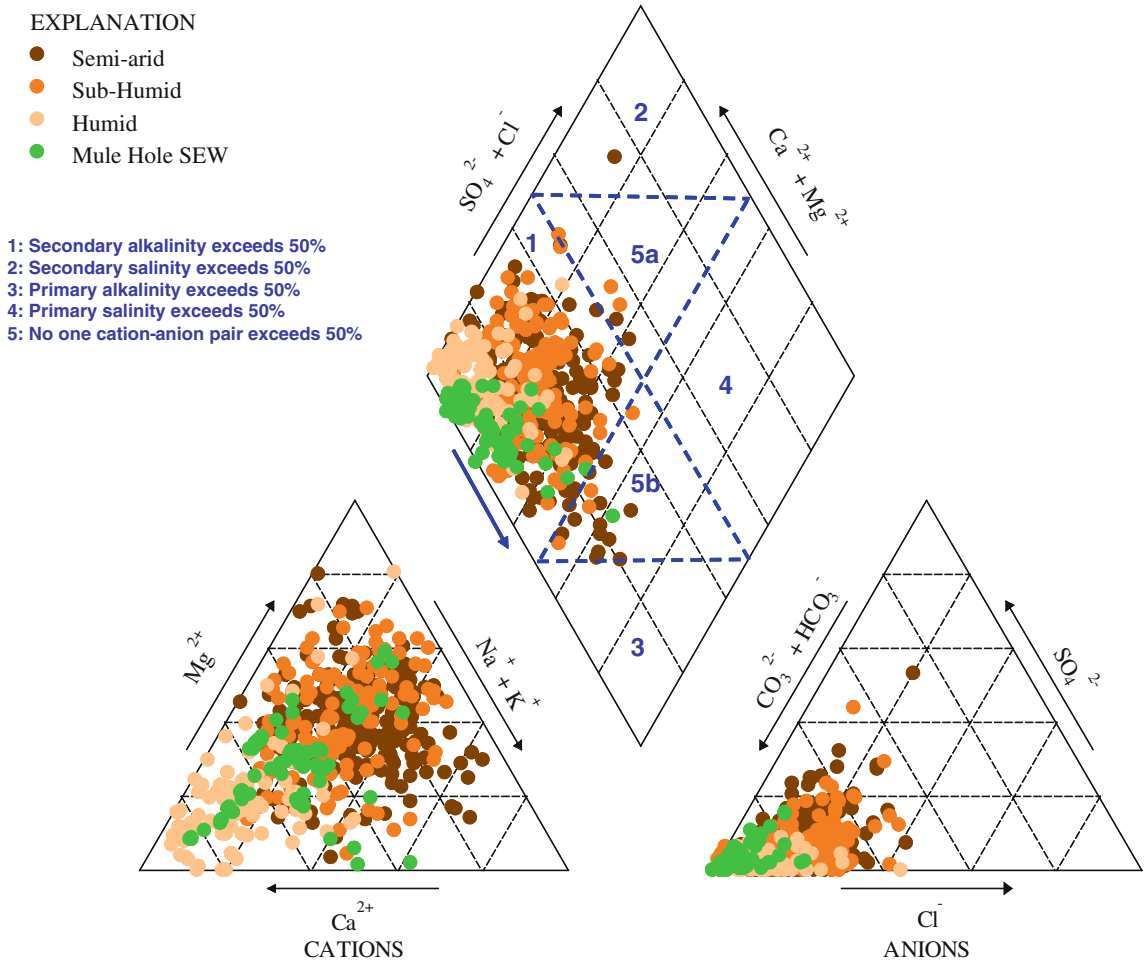

Fig. 6 Piper's diagram showing the evolution of groundwater

2008). Molar ratio of Na:Cl is ~1 in the Upper Kabini basin (humid zone). Thus, the total amount of Cl^- is related to Na^+ and the only source for both marine elements is evaporation of rainwater (Carrillo-Rivera et al. 2007). Na/Cl >1 in some samples of semi-arid and transition zones indicates that excess of Na^+ is due to *ion exchange*. Exchange is between water and some minerals notably clayey ones that are present within the aquifer matrix (Guendouz et al. 2006). Excess of Na might also be contributed from *leaching of fluid inclusions* and/or silicate weathering. Samples of monsoon period with mNa/Cl <1 generally correspond to waters affected by the contribution of precipitation (recent recharge). Most of the non-monsoon samples in semi-arid zone have high Cl^- which is contributed by evaporation. m$(Ca^{2+} + Mg^{2+})/Cl^-$ is >1 for all the samples of the three zones supporting reverse ion exchange process. Na^+ exchange for Ca^+ and Mg^{2+} and calcite precipitation also contribute to water composition (Zhu et al. 2008) and are good indicators of groundwater flow (Carrillo-Rivera et al. 2007). It is confirmed that Ca^{2+} and Mg^{2+} solely originate from dissolution of soil and rock in the semi-arid zone and from *weathering of accessory pyroxenes and amphibole minerals* based on $(Ca^{2+} + Mg^{2+})/HCO_3^-$ molar ratio (~0.5) (Kumar et al. 2006). HCO_3^- >200 mg/L is observed in the sub-humid and semi-arid zones. Possible sources of such high quantities of HCO_3^- include presence of organic matter in the groundwater, which gets oxidized to produce CO_2 gas, which in turn promotes dissolution of minerals. This weathering further enriches the concentrations of Ca^{2+}, Mg^{2+} and HCO_3^- in groundwater. Weathering of silicate minerals can also act as a source of HCO_3^-.

In summary, some Na may be derived from Na-bearing silicate minerals, such as albite weathering producing kaolinite and Na^+ ions. A part of the Na^+ and Ca^{2+} is produced by the breakdown of plagioclase, specifically oligoclase (Braun et al. 2009). Another part of the Ca comes from calcite dissolution (Hidalgo and Cruz-Sanjulian 2001). K^+ and Mg^{2+} are produced by the dissolution of micas and chlorite. HCO_3^- is produced from CO_2 gas, which comes either from atmosphere or from calcite. Al^{3+} and SiO_2^- come from the combination of all these minerals

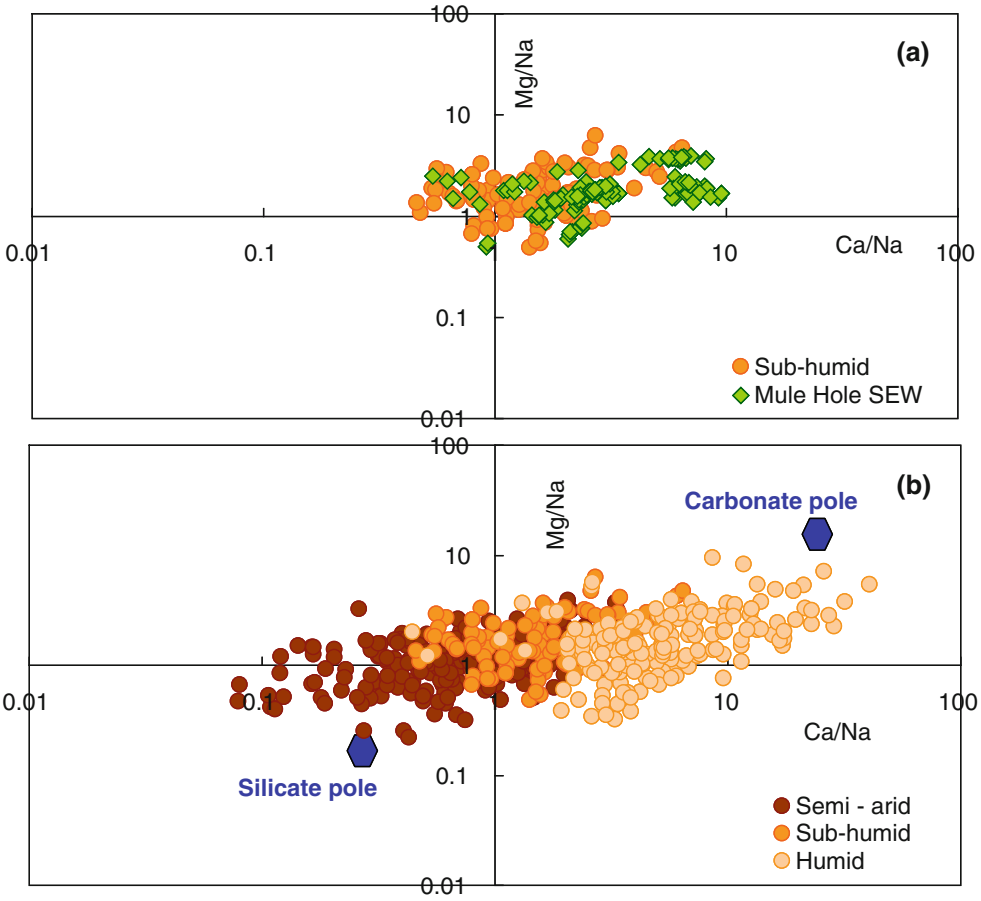

Fig. 7 Ca/Na versus Mg/Na plot for groundwater of **a** Mule Hole SEW in sub-humid zone and **b** the three climatic zones

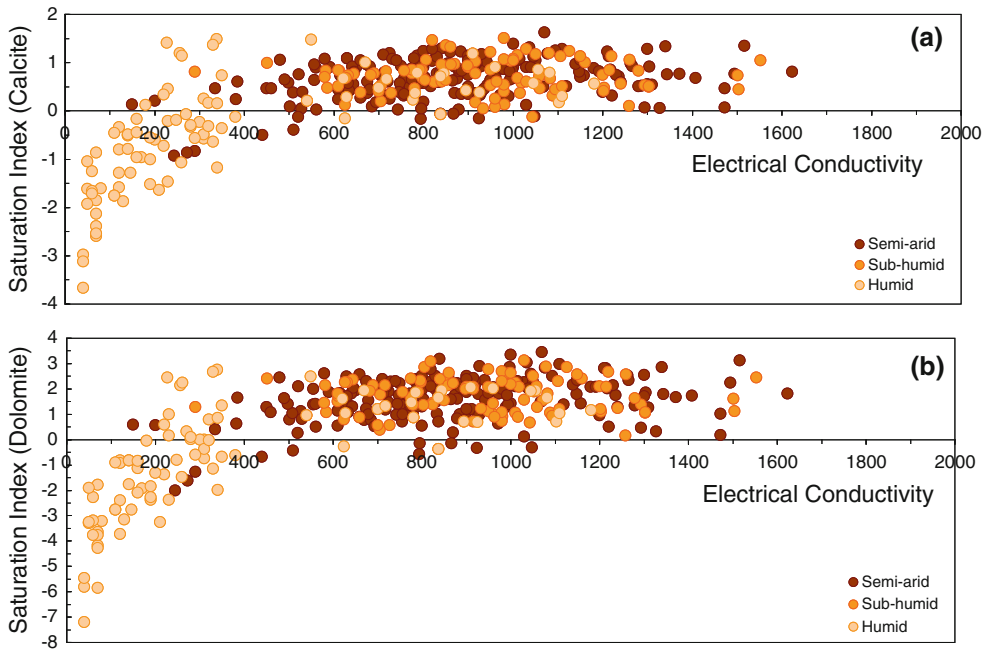

Fig. 8 Saturation indices of **a** calcite and **b** dolomite observed for the study area

and are immediately fixed in the insoluble phases. Further, the weathering of primary and secondary minerals also contributes cations and silica in the system (Grimaud et al. 1990). Thus, Cl^- and Na^+ originate from rain and all other ions, HCO_3^-, Ca^{2+}, Mg^+, K^+ and SO_4^{2-}, originate from water rock interactions.

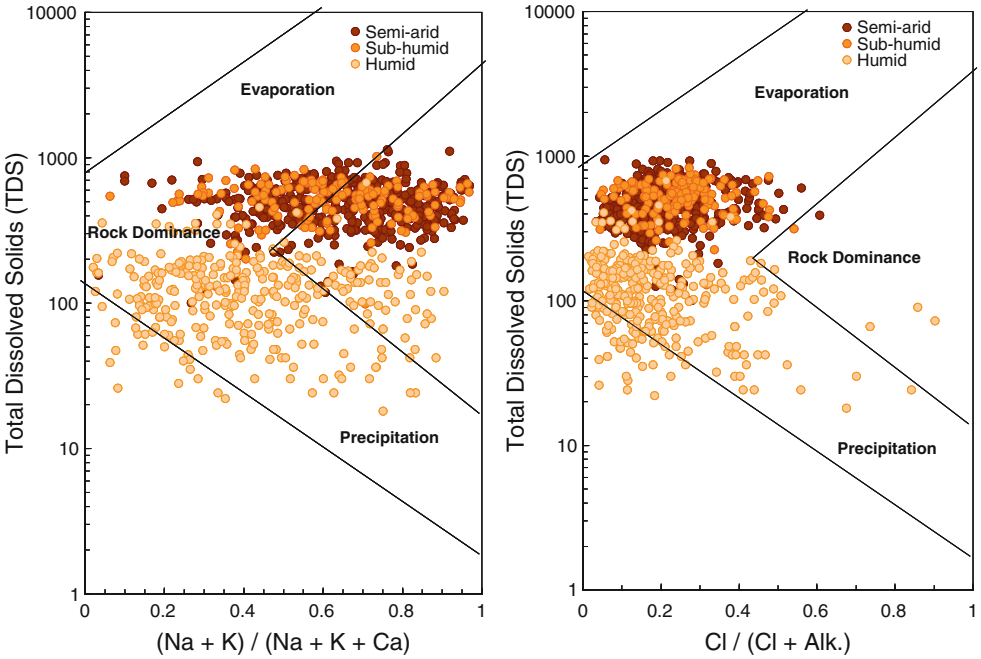

Fig. 9 Gibbs's diagram for the study area

Concentration–depth profiles

Concentration–depth profiles are plotted for individual ions in some of the wells to identify the prominent ions and their conservative behavior (Broers and Van der Grift 2004). K^+ does not vary much with depth since it appears in the groundwater due to throughfall and thus becomes nominal at greater depths. Ca^{2+} is observed to remain almost in the same range for the three zones. Thus, Ca^{2+} is least affected by change in rainfall pattern and varies with the amount of weathering process. Hence, Ca^{2+} and K^+ are eliminated in the concentration–depth profiles shown in Fig. 10. Approximate depths of different stratified layers for the study region are also shown in the figure.

It is observed from the figure that Na^+, Cl^-, SO_4^{2-} and Mg^{2+} show increase/decrease with each stratified layer. Concentration of all these four ions increases with depth in the top 15 m layer in the semi-arid and sub-humid zones, while there is a decreasing trend for the humid zone. At the top surface, dilution and leaching of rainwater in the humid zone causes decrease in concentrations. Weathering producing the end product elements further increases/decreases the concentrations in the saprolite layer (10–17 m). Concentration increase trends in sub-humid and semi-arid zones and the decrease trends in the humid zone are retained in the saprolite layer. Weathering process occurs at a lower rate in the layers below. Hence, in the fractured zone (17–25 m below ground level), the concentrations

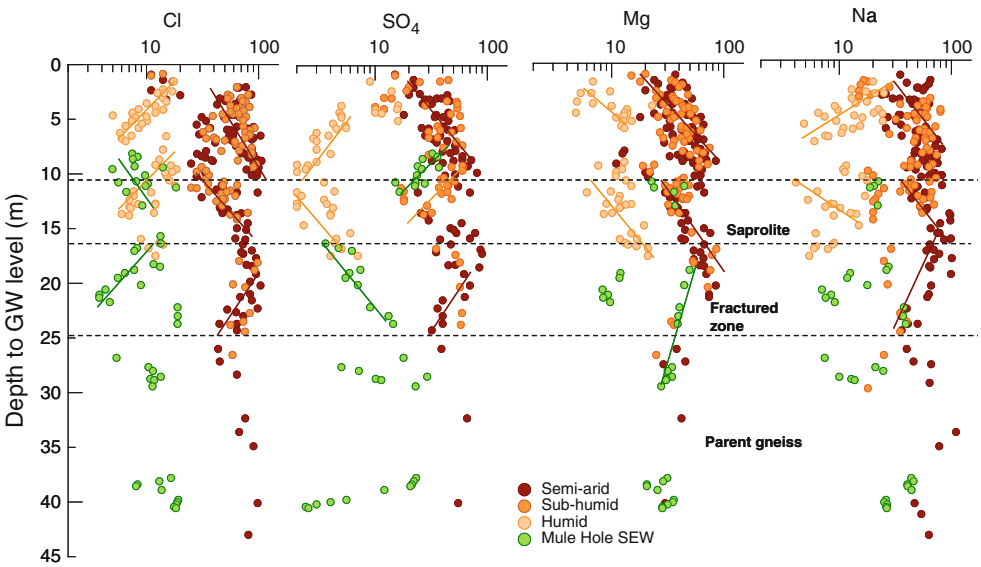

Fig. 10 Concentration–depth profiles for the study area

decrease with the increase in depth. Further, in the parent gneiss zone (>25 m), concentration variations with depth are not observed much.

Mule Hole SEW, located in the transition sub-humid zone is observed to obey the trend of rest of the sub-humid zone, same as observed in Fig. 7a. A lateral shift in the concentrations of all ions on the higher side is observed in the semi-arid and sub-humid zones (Fig. 10). These higher concentrations of Cl^- and Na^+ in semi-arid zone (low rainfall) and lower concentrations in humid zone (high rainfall) indicate the amount of input received from rainwater (Soumya et al. 2009). Mg^{2+} and SO_4^{2-} are generated in the matrix as a result of weathering in the semi-arid and sub-humid zones, which increase their concentrations. Hence, it can be deduced that concentration variations with depth are influenced by the geological stratifications observed in the region.

'Deep' and 'shallow' wells

Since the mineralogy of the region changes at deeper levels and has an impact on the quality of groundwater, classification of all the wells into 'deep' and 'shallow' categories is essential to differentiate them in terms of the depth of occurrence of groundwater. Depth to water table in humid zone is shallow (10 m) while in semi-arid zone it reaches 30 m. On the other hand, depth to hard rock in humid zone is at 20 m and in semi-arid zone it is at 10 m. Hence, most of the wells in humid zone fluctuate in completely weathered laterites and do not reach deeper hard rock (gneiss at 20 m). Lesser rainfall (800–1,200 mm) in semi-arid zone, which is subject to continuous human pumping, results in deeper groundwater (35–40 m). Based on this, an average of 12 m is considered to be the criteria for shallowness i.e., wells in which mean groundwater depth (h) is <12 m are considered as 'shallow' wells. Other wells whose mean groundwater depth is >12 m are considered as 'deep' wells.

Hydrological classification into groups based on groundwater fluctuations

Variations in groundwater levels at different depths result in interactions with different type of rocks each time at every depth and thus result in different chemical signatures. Based on the groundwater fluctuation criteria, the wells at Mule Hole SEW were classified into the four groups by Maréchal et al. (2009). Mineralogy of Mule Hole SEW was studied by Braun et al. (2009) and it is observed that classification into four groups based on hydrology was a reflection of mineralogical differences observed at several depths. Depth and extent of weathering were observed to be strongly correlated among the four defined classes (Soumya et al. 2011). Similar analysis is carried out for the entire study area to study the correlation between groundwater fluctuations and its corresponding chemistry.

Variations in water level fluctuations are studied initially to classify the study area into different groups. Monthly fluctuations were estimated for ith well during every 'm' month as Δh_i^m using the below equation:

$$\Delta h_i^m = \mathrm{GW}_i^{m+1} - \mathrm{GW}_i^m \,(\text{ground water level}) \Delta h_i^{t,\max} = \Delta h_i^{\mathrm{pre},\max} - \Delta h_i^{\mathrm{post},\max} \qquad \overline{\Delta h_i} = \sum_{n=1}^{t} \Delta h_i^{t,\max} / t \qquad (3)$$

where Δh_i^m is monthly groundwater fluctuation for ith well, $\Delta h_i^{\mathrm{pre},\max}$ is maximum monthly groundwater fluctuation for pre-monsoon period during a year for ith well, $\Delta h_i^{\mathrm{post},\max}$ is maximum monthly groundwater fluctuation for post-monsoon period during a year for ith well, $\Delta h_i^{t,\max}$ is maximum fluctuation for the year t at ith well, $\overline{\Delta h_i}$ is mean of all these maximum fluctuations over the entire t year period for ith well.

Mean of these fluctuations over $n = 1$ to t years gives the mean picture of temporal behavior for every well. Based on these Δh values, all the wells are classified into four classes defined as (Maréchal et al. 2009):

$$\text{Group I} : \overline{\Delta h_i} < 2 \text{ m} \quad \text{Group II} : 2 \le \overline{\Delta h_i} < 4.5 \text{ m}$$
$$\text{Group III} : 4.5 \le \overline{\Delta h_i} < 6.5 \text{ m} \quad \text{Group IV} : \overline{\Delta h_i} \ge 6.5 \text{ m}$$

This classification is applied for the uncontaminated wells of Table 2 in the basin. Most of the wells in the basin belong to 'group II' category with eastern end of the basin falling under 'group III'. Most of the wells fluctuating <2 m can be said to be either dormant or being recharged annually maintaining the water level. Dormant wells do not show any chemical variations while recharged wells show a wide variation in chemistry. Wells belonging to 'Group II' react hydraulically to the annual rainfalls and show moderate fluctuations. 'Group III' wells show higher fluctuations indicating that these fluctuations might be due to either stratigraphy or anthropogenic affect. 'Group IV' consists of wells fluctuating by more than 6.5 m. High specific yield of the aquifer (stratigraphy) or pumping (anthropogenic effect) are the reasons for these high groundwater fluctuations. Groundwater in few other wells fluctuate among all the layers i.e., from top regolith to deep hard rock layers. Hence, mean annual ground water fluctuations ($\overline{\Delta h_i}$) and the mean depth to groundwater (h, as described in "Mineralogical interactions") are considered as the criteria for classification of the wells.

Hence the criteria adopted for classification of wells based on mean annual depth (h) and mean annual fluctuation ($\overline{\Delta h_i}$) are shown in Table 3. It is observed that all the

Table 3 Criteria for classification of wells into groups

Classification	Mean groundwater depth (h) (m)	Mean annual fluctuation (Δh) (in m)
Group I	<12	<2.5
Group II A	<12	2.5–4.5
Group II B	>12	2.5–4.5
Group III A	<12	4.5–6.5
Group III B	>12	4.5–6.5
Group IV	>12	≥6.5

wells of 'group I' are 'shallow' and of 'group IV' are 'deep'. 'Group II A' category shows medium fluctuations ($2 \leq \overline{\Delta h_i} < 4.5$ m) at shallow depths. Few places in group II are subjected to pumping reaching deeper water levels and are categorized in 'group II B'. Groundwater fluctuations in the third group reach as high as 6.5 m especially in regions where the rainfall is low (mainly semi-arid zone). Constant pumping or low specific yield results in these high water level fluctuations. 'Shallow' (group III A) and 'deep' (group III B) classification in the third group is influenced by the local mineralogy of the well. Some of these wells which are initially shallow reach deeper levels due to continuous usage. 'Group IV' wells have very high fluctuations subject to both low specific yield and high pumping. Fluctuations in these fourth group wells traverse among all the layers from top weathered zone to deeper hard rock layers. Hence, all the 'group IV' wells can be considered as 'deep' without any further classification.

All the wells of the study area are thus classified into these six classes as given in Table 4. Some of the wells, which were shallow in initial periods (in 1990s) have become deep in the recent times due to continuous extraction. They are included in both 'shallow' and 'deep' categories (marked as * in Table 4). In such wells a part of the data is at shallow depths while the data pertaining to later periods will be at deeper levels. Such wells are observed more in groups III B and IV categories with moderate/high groundwater fluctuations. Climatic effect of the groundwater chemistry is studied in the next section for each of these categories.

Discussion

Concentrations of Ca^{2+} and Mg^{2+} in groundwater are due to water rock interactions. Na in humid zone comes

Table 4 Classification of wells of the study area into different groups

Taluk	Group I	Group II		Group III		Group IV
	I	II A (Shallow)	II B (Deep)	III A (Shallow)	III B (Deep)	IV
Semi-arid zone						
Chamarajnagar (C)		C9		C7	C3*, C5*, *C8*	C11*, C16*
Gundlupet (G)		G2*, *G5*, G6	*G1*		C13*	
Kollegal (Ko)			*Ko4*	Ko3*	*G3**	
K. R. Nagar (KR)	KR2	KR7		*KR3*, KR5	Ko2*	
Nanjangud (N)	N1	*N2*, N3, N6, *N7*, N9				
Periyapatna (P)					N10, *N11*	*P4*
T. Narasipur (TN)		TN6, *TN7*		*TN1*		
Mysore (My)					My8	
Sub-humid zone						
H. D. Kotte (HD)		HD1, HD10, HD6*, *HD9, HD11*	*HD3*, HD4		*HD2,* HD7	*H9*
Hunsur (H)		*H5*	*H7*			
Periyapatna (P)		*P7*				
Gundlupet		G9				
Humid zone						
Kalpetta (K)	K10	K1, K4, *K6, K7*, K9	*K3**	K8		
Mananthavady (M)	M1	*M2*, M3, M4, *M9*	M5	*M8*		
Sulthanbathery (S)	S1, S4, S6		S3*	*S7, S10*		
H. D. Kotte (HD)		HD8				
Mule Hole SEW	MH3, MH5, MH6	MH2, MH8, MH10, MH12, MH13	MH9			

* Wells which are both shallow and deep during the study period. Categorisation is based on the group to which they belong for the maximum period during the study

Italics and underlined wells exhibit anti-dilution behaviour "Dilution: anti-dilution concept for seasonal patterns"

entirely from atmosphere but in semi-arid a part of Na^+ is contributed by silicaceous rocks and another from atmospheric contribution (Carrillo-Rivera et al. 2007). As observed in Fig. 7b, Ca/Na ratio varied by more than 10 times in the semi-arid zone, receiving low rainfall. This can be accounted for alternate dry–wet bimodal rainfall pattern. Humid zone, which receives highest rainfall, experiences small range of Ca/Na values (<5 times). This consistency can be due to unimodal rainfall pattern in the zone. Mg/Na ratio is same for the whole zone except for few high values in humid zone (might be due to low Na^+). Variation in Ca/Na ratio is due to high Ca^{2+} concentrations in pore water of humid zone. Ca^{2+} in semi-arid zone is mainly in the form of carbonate nodules resulting in very low concentrations in pore water. The proportion of Na^+ from weathering is nominal in the humid zone while it is high in the semi-arid zone resulting in very low values of Ca/Na and Mg/Na. Further, observed high Mg/Ca ratios in this zone strongly indicate weathering of carbonates containing high concentrations of Mg, which is common in wet zones of river basins (Zhu et al. 2008).

Carbonates versus silicates along the climatic gradient

2D representation of new '3D block plot' (Soumya et al. 2008) is used here for classifying chemistry at individual well scale. In this technique, *y* axis shows Ca/Cl for 'carbonates' and *x* axis represents Na/Cl ratio—a representation of 'Na-silicates'. Initially both shallow and deep wells are plotted in Fig. 11 to check for variations at regional scale under the influence of rain. On the whole shallow wells of all the three zones have low molar ratios as a result of dilution from the rainfall (Fig. 11a). Deeper wells have higher molar ratios due to undisturbed accumulation of concentrations (Fig. 11b).

As the rainfall increases along the gradience in the basin, groundwater becomes more carbonaceous and varies along Ca/Cl ratios. Reduction in Na-silicates with the increase in rainfall (from semi-arid to humid) is observed in both shallow and deep wells. Except for some points, sub-humid zone behaves in the intermediate fashion. Variance in data for humid zone spreads along 'carbonate axis' (*y* axis) while that for semi-arid zone spreads along 'silicate axis' (*x* axis). Variability in Ca/Cl and Na/Cl ratios is higher for the shallow wells (Fig. 11a) and slightly lower for the deep wells (Fig. 11b). Wide spread in data (high variance) in both directions (along Ca/Cl and Na/Cl axes) is observed for sub-humid zone (Fig. 11). This variability in the three climatic zones are further analyzed by studying the temporal (monsoon–non-monsoon) patterns for every individual well.

Dilution: anti-dilution concept for seasonal patterns

Classification into seasonal cycles (Kumar et al. 2006), identified in most of the investigations, was so far done crudely on the basis of monsoon–non-monsoon periods. This crude classification was successful in humid zone receiving unimodal rainfall. Results of this classification for semi-arid zone were ambiguous since the region received rains twice a year (bi-modal rainfall). Further, deeper wells could not show clear difference between dry and wet periods because of the time lag in actual recharge. Droughts and flood periods worsened the interpretations. A new method is adopted here to identify the actual monsoon months based on 'rainfall intensity'. Period of a year having higher

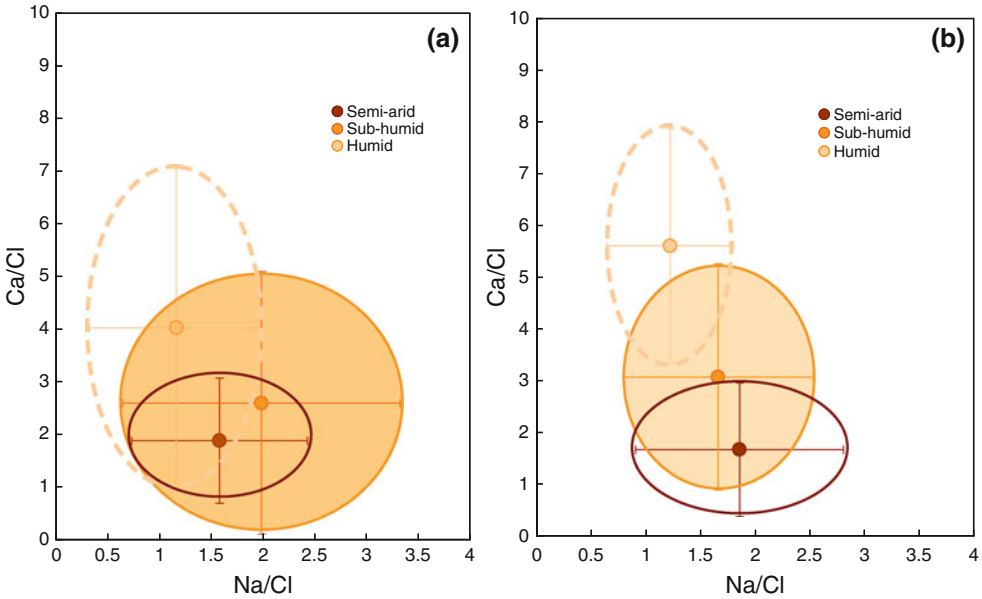

Fig. 11 Carbonates versus silicates along the climatic gradient for **a** shallow wells and **b** deep wells

rainfall shows diluted chemistry and this chemistry was compared with dry period. In contrast, some of the wells showed dilution chemistry (lower concentrations) during dry season, when compared to wet season. Hence, analysis on this basis is known as 'dilution principle' for the former case and 'anti-dilution principle' for the latter case.

Average rainfall for Mule Hole SEW is around 96 mm/month while that in humid and semi-arid zones is approximately 70 and 200 mm/month, respectively. Monsoon period of some years did not receive enough rainfall (drought periods) and non-monsoon months during some years received higher rainfall (delay in rains). It was observed that months having rainfall more than these threshold values contributed to recharge at local scale. Only these months can be considered for 'recharge period' analogous to 'monsoon' while others cause discharge as during non-monsoon. The effect of recharge is usually observed after 30 days (residence time for the area). Hence, chemistry of samples collected after this residence time showed the actual recharge affect (dilution chemistry). Chemistry, in terms of Na/Cl and Ca/Cl molar ratios, supports this principle. Data is classified into 'recharge period' and 'discharge period' based on the following chemical signatures:

a) Dilution principle:

Normal recharge/discharge:

Recharge → Sufficient rainfall + GW changes + Dilution chemistry

Recharge ± pumping: recharge occurs but pumping causes deep levels

Recharge → Sufficient rainfall + High GW fluctuations + Dilution chemistry

b) Anti-dilution principle:

No/insufficient recharge ± pumping effect: rain could not reach deep GW layers and discharge period continues during rainy months also.

Discharge → Insufficient rainfall + GW declines + Anti − Dilution chemistry

Anti-dilution' concept. 'Group IV' wells are omitted in this temporal analysis. All the five groups are classified into the above said three classes (dilution–anti-dilution):

Dilution	Normal recharge/discharge → group I, group II A Recharge + pumping → group II B, group III A, group III B
Anti-dilution	No recharge + pumping → group II A, group II B, group III A, group III B

It is observed that most of the 'group I' and 'group II A' (shallow) wells exhibit the normal dilution principle since they are recharged annually maintaining the groundwater levels. Deep wells of 'group II' (II B) show anti-dilution chemistry. All the wells of 'group III' (III A and III B) category show anti-dilution chemistry since pumping continues even in low rainfall periods. This results in almost no recharge and in higher concentrations (anti-dilution chemistry). Apart from this general behavior some of the shallow wells show anti-dilution behavior, may be due to local chemical changes.

Sodium–carbonate plots of Fig. 11 are plotted for the wells showing both dilution and anti-dilution behavior (contrasting chemistry) under each of the four groups. Classification into shallow and deep wells is continued for this analysis so as to check for the influence of chemistry at different depths.

Case (a): dilution chemistry

Sufficient rainfall events occurring periodically cause recharge in groundwater. In the absence (or negligible affect) of human intervention (pumping), groundwater levels do not fluctuate much. In the dry period of the same year, this recharge gets drained into neighboring deficit areas causing discharge. Generally, groundwater during discharge periods has higher mineral concentration compared to that at the recharge periods due to the longer residence time and prolonged contact with the aquifer matrix, in accordance with dilution concept (Kumar et al. 2006). Silicate–carbonate plot for dilution scenario is plotted for both shallow and deep wells as shown in Fig. 12.

In general, wells of semi-arid zone are silicaceous while that of humid are carbonaceous (high variance along *y* axis of Fig. 12). Sufficient recharge takes place in these wells. Few shallow wells of semi-arid zone show minimum groundwater fluctuations and have low molar ratios of Na/Cl and Ca/Cl (Fig. 12a). Similarly, some of the deep wells in sub-humid zone, which are fluctuating at >4.5 m (groups I, II A), exhibit dilution chemistry. All the shallow wells of humid zone belonging to groups I, II A and II B showed dilution chemistry due to continuous input from rain. 'Shallow' wells of semi-arid zone fluctuating at ≤4.5 m (groups I and II A) and some 'deep' wells of the zone fluctuating at 4.5–6.5 m (group III B) show similar chemistry, i.e., mean ± standard deviations of Ca/Cl and Na/Cl ratios are same (Fig. 12a, b). Drainage network in the region between Upper Cauvery and Kabini (sub-humid zone) alters the chemistry of groundwater. Most of the deeper wells do not always

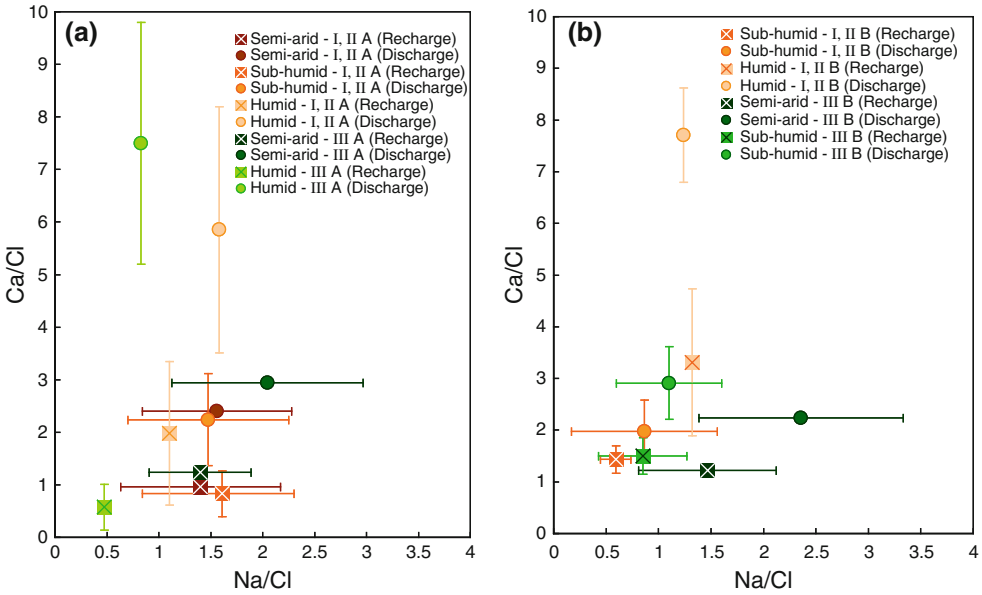

Fig. 12 Dilution chemistry for **a** shallow wells and **b** deep wells

receive the entire rainfall (in terms of magnitude) and actual recharge does not take place. Pumping during such periods adds to decline in groundwater levels and a different chemistry.

Case (b): anti-dilution chemistry

When the water level rises up to the weathered layer (in hard rock formations of deep wells), the concentrations of the major ions increase due to dissolution of minerals deposited during the preceding dry season, ion-exchange processes and ions derived from anthropogenic activities, especially from agricultural activities (Jankowski and Acworth 1997; Rao and Rao 2010). During lowering of the water level, the concentration of ion decreases due to the re-deposition of minerals and adsorption of ions thus reflecting the 'anti-dilution' principle as shown in Fig. 13. Concentration increase induces cation exchange due to evapotranspiration, whereby Ca^{2+} on the soil exchanger is replaced by Na^{+} (Stigter et al. 1998). Further, small showers after these prolonged dry periods push the vadose zone concentrations to deeper water levels causing increase in chemistry during recharge period reflected by higher molar ratios (Fig. 13). As the input rain continues for some more time (even though the magnitude of rainfall is less) the chemistry gets diluted later at the end of monsoon or sometimes even in non-monsoon period depending on the residence time for the groundwater in that region. This

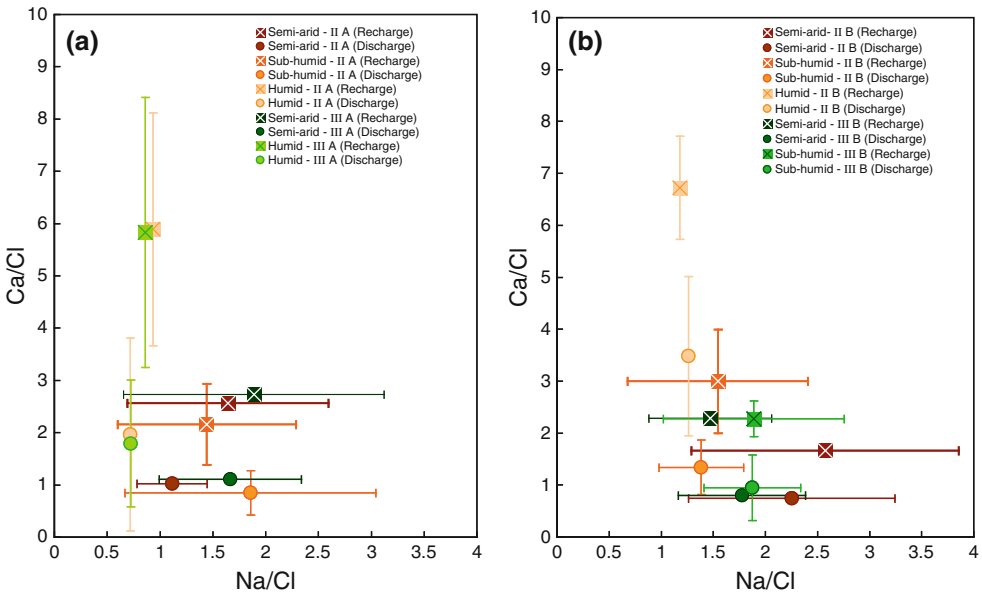

Fig. 13 Anti-dilution chemistry for **a** shallow wells and **b** deep wells

contrast behavior is reflected by low molar ratios corresponding to dry season and physically by high positive Δh values (Fig. 13). Wells which exhibit anti-dilution chemistry are enlisted in Table 4 (italics, underlined wells)

Though the wells under groups I and II fluctuate <4.5 m, anti-dilution chemistry is observed in some of the wells (Fig. 13a) with diluted chemistry during dry season and higher chemistry during recharge period. This is observed only in sub-humid and semi-arid zones. High fluctuations (group III) are observed in this semi-arid zone since groundwater extraction is more despite of low rainfall resulting in anti-dilution chemistry. Most of the wells (both shallow and deep) in the semi-arid zone are under 'group III' exhibiting anti-dilution chemistry (Fig. 13b). Very few wells from humid zone, fluctuating more than 6.5 m annually, show this contrasting chemistry. Thus, classification of the region based on 'recharge–discharge' concept would assist in identifying the zones which are not recharged actually. It helps in demarcating the deeper wells which are naturally deep and get recharged from wells affected by pumping.

Conclusions

As the groundwater migrates through the porous media, the composition may be altered due to interactions with the various mineral phases present in the naturally heterogeneous weathered matrix. An experimental watershed, Mule Hole SEW is considered for analyzing the hydrogeochemical behavior of groundwater at local scale, which is further extended to the climatic zones on either side. Groundwater chemistry along the three climatic zones is observed to be less polluted (<40 % of pollution percentage) but is high in Ca–Mg hardness (TH > 180 mg/L). Hydrochemical facies identified in this study are $CaHCO_3$ in humid zone, which evolved into $CaNaHCO_3$ in semi-arid zone.

At local scale, hydrochemical behavior of Mule Hole SEW is a representative and can be upscaled to the entire sub-humid zone. Further, it is observed from molar cation ratio plot that the sub-humid zone transits chemically between the semi-arid and humid zones. Ca/Na ratio varies by more than 100 times from the semi-arid (bimodal rainfall) to humid zones (unimodal rainfall), which is mainly due to both climatic and lithological controls. Ion exchange processes cycling exists between Cl^- and SO_4^{2-} and between Ca^{2+} and Na^+. Silicate weathering produce excess of Na^+ in the groundwater. Evaporation increases the Cl^- content during dry period. Dissolution/precipitation of primary/secondary calcite, weathering of accessory pyroxenes and amphibole minerals contribute for Ca^{2+} and Mg^{2+} in the groundwater. K^+ is produced by dissolution of biotite and K-feldspar. Groundwater chemistry was increasing with depth and is observed to vary with geological stratification (~18 m of saprolite; ~25 m of fracture rock with parent gneiss beneath).

Wells in the study area are classified into 'deep' and 'shallow' based on the depth at which groundwater fluctuates with 10 m as the benchmark for shallowness. Further, the wells could be classified into four groups based on the magnitude of fluctuations (Δh). Variation in groundwater chemistry in these four groups is due to change in both Δh and mineralogy. Hence, these chemical variations are analyzed for the seasonal patterns.

Ca/Cl versus Na/Cl (2D plots) indicates semi-arid zone as more silicaceous while humid zone is more carbonaceous. This might be due to a possible lithologic control in the three climatic zones, i.e. Ca-rich parent rocks could be more abundant in humid zone than in the semi-arid zone, dominated by Na-plagioclase. Sub-humid zone has shallow wells showing humid zone pattern and deep wells showing semi-arid zone pattern. Based on the amount of rainfall and type of rainfall, samples are classified into 'recharge–discharge' periods unlike traditional 'monsoon–non-monsoon' periods. All wells have lower Na/Cl and Ca/Cl ratios during recharge period than during discharge period and obey dilution principle. Wells obeying dilution principle are termed as 'normal' and those under the influence of pumping show anti-dilution behavior—low molar ratios during discharge periods. Pumping accompanied by continuous recharge during monsoon periods retains the dilution chemistry principle. Insufficient recharge either due to drought or due to deepness of the wells causes the anti-dilution chemistry. Most of the wells with low water level fluctuations show dilution chemistry while with high fluctuations (mostly in semi-arid zone) show anti-dilution chemistry. Application of both physical (water level fluctuations) and chemical concepts on groundwater at well scale helps in characterizing the region into different categories which are distinct among themselves. This preliminary analysis is a basis for understanding hydrogeochemical behavior of the basin.

Acknowledgments Kabini river basin is analyzed as a part of ORE-BVET project (Observatoire de Recherche en Environnement-Bassin Versant Expérimentaux Tropicaux, http://www.orebvet.omp.obf-mip.fr). Apart from the specific support of French Institute of Research for Development (IRD), Embassy of France in India and Indian Institute of Science, our project is funded by IRD, INSU/CNRS (Institut National des Sciences de l'Univers/Centre National de la Recherche Scientifique) and IFCPAR (Indo-French Center for the Promotion of Advanced Research W-3000) through the French program ECCO-PNRH (Ecosphère Continentale: Processus et Modélisation-Programme National Recherche Hydrologique). The multidisciplinary research at Mule Hole watershed began in 2002 under the aegis of the IFCWS (Indo-French Cell for Water Sciences), a joint laboratory IISc/IRD. We thank Karnataka Forest Department and the staff of Bandipur National Park for all the facilities and support they

provided. We also thank the staff of Department of Mines and Geology (DMG), Karnataka and the Groundwater Department of Kerala for providing us with all kinds of data as and when required. Their enormous interest in our research encouraged us to complete this work.

References

APHA-WWA-WPCF (1998) Standard methods for the examination of water and wastewater, 20th edn. Am Public Health Assoc (APHA), Baltimore

Arumugam K, Elangovan K (2009) Hydrochemical characteristics and groundwater quality assessment in Tirupur Region, Coimbatore District, Tamil Nadu, India. Environ Geol 58(7):1509–1520

Ayraud V, Aquilina L, Labasque T, Pauwels H, Molenat J, Pierson-Wickmann A-C, Durand V, Bour O, Tarits C, Pierre LC, Fourre E, Merot P, Davy P (2008) Compartmentalization of physical and chemical properties in hard-rock aquifers deduced from chemical and groundwater age analyses. Appl Geochem 23(9):2686–2707

Barbiero L, Parate HR, Descloitres M, Bost A, Furian S, Mohan Kumar MS, Kumar C, Braun J-J (2007) Using a structural approach to identify relationships between soil and erosion in a non-anthropic forested area, South India. Catena 70:313–329

Bertolo R, Hirata RH, Sracek O (2006) Geochemistry and geochemical modeling of unsaturated zone in a tropical region in Urania, Sao Paulo state, Brazil. J Hydrol 329(1–2):49–62

Bharadwaj V, Singh DS (2011) Surface and groundwater quality characterization of Deoria District, Ganga plain, India. Environ Earth Sci 63(2):383–395

Bharadwaj V, Singh DS, Singh AK (2010) Hydrogeochemistry of groundwater and anthropogenic control over dolomitization reactions in alluvial sediments of the Deoria district: Ganga plain, India. Environ Earth Sci 59(5):1099–1109

BIS (1991) Bureau of Indian Standards—Indian Specification for Drinking Water IS: 10500

Braun J-J, Descloitres M, Riotte J, Fleury S, Barbiero L, Boeglin J-L, Violette A, Lacarce E, Ruiz L, Sekhar M, Mohan Kumar MS, Subramanian S, Dupre B (2009) Regolith mass balance inferred from combined mineralogical, geochemical and geophysical studies: Mule Hole gneissic watershed, South India. Geochem Cosmochim Acta 73(4):935–961

Broers HP, Van der Grift B (2004) Regional monitoring of temporal changes in groundwater quality. J Hydrol 296(1–4):192–220

Carrillo-Rivera J-J, Varsanyi I, Kovacs LO, Cardona A (2007) Tracing groundwater flow systems with hydrogeochemistry in contrasting geological environments. Water Air Soil Pollut 184(1–4):77–103

Descloitres M, Ruiz L, Sekhar M, Legchenko A, Braun J-J, Mohan Kumar MS, Subramanian S (2008) Characterization of seasonal local recharge using electrical resistivity tomography and magnetic resonance sounding. Hydrol Process 22(3):384–394

Durand N, Gunnell Y, Curmi P, Ahmad SM (2007) Pedogenic carbonates on Precambrian silicate rocks in South India: origin and paleoclimatic significance. Quat Int 162–163:35–49

Fantong WY, Satake H, Ayonghe SN, Aka FT, Asai K (2009) Hydrogeochemical controls and usability of groundwater in the semi-arid Mayo Tsanaga River Basin: far north province, Cameroon. Environ Geol 58(6):1281–1293

Galuszka A (2007) A review of geochemical background concepts and an example using data from Poland. Environ Geol 52(5):861–870

Gibbs RJ (1970) Mechanism controlling world's water chemistry. Science 170:1088–1090

Grimaud D, Beaucaire C, Michard G (1990) Modeling of the evolution of groundwater in a granite system at low temperature: the Stripa groundwater, Sweden. Appl Geochem 5:515–525

Guendouz A, Moulla AS, Remini B, Michelot JL (2006) Hydrochemical and isotopic behavior of a Saharan phreatic aquifer suffering severe natural and anthropogenic constraints (case of Oued-Souf region, Algeria). Hydrogeol J 14(6):955–968

Guler C, Thyne GD, McCray JE, Turner AK (2002) Evaluation of graphical and multivariate statistical methods for classification of water chemistry data. Hydrogeol J 10:451–455

Gunnell Y (1998a) Passive margin uplifts and their influence on climatic change and weathering patterns of tropical shield regions. Global Planet Change 18:47–57

Gunnell Y (1998b) Present, past and potential denudation rates: is there a link? Tentative evidence from fission-track data, river sediment loads and terrain analysis in the South Indian shield. Geomorphology 25:135–153

Gunnell Y (2000) The characterization of steady state in Earth surface systems: findings from the gradient modelling of an Indian climosequence. Geomorphology 35:11–20

Gunnell Y, Bourgeon G (1997) Soils and climatic geomorphology on the Karnataka plateau, peninsular India. Catena 29:239–262

Gunnell Y, Radhakrishna BP (2001) A survey of soils and weathering patterns through land system mapping in the Western Ghats region. In Sahyadri—the great escarpment of the Indian subcontinent. Geol Soc of India. Memoir 47 (1 and 2), pp 1054

Gunnell Y, Gallagher K, Carter A, Widdowson M, Hurford AJ (2003) Denudation history of the continental margin of western peninsular India since the early Mesozoic—reconciling apatite fission-track data with geomorphology. Earth Planet Sci Lett 215:187–201

Gunnell Y, Braucher R, Bourles D, Andre G (2007) Quantitative and qualitative insights into bedrock landform erosion on the South Indian craton using cosmogenic nuclides and apatite fission tracks. Geol Soc Am Bull 119:576–585

Hidalgo MC, Cruiz-Sanjulian J (2001) Groundwater composition, hydrochemical evolution and mass transfer in a regional detrital aquifer (Baza basin, southern Spain). Appl Geochem 16(7–8): 745–758

Jalali M, Khanlari ZV (2008) Major ion chemistry of ground waters in the Damagh area, Hamadan, western Iran. Environ Geol 54(1):87–93

Jankowski J, Acworth RL (1997) Impact of debris flow deposits on hydrogeochemical processes and the development of dry land salinity in the Yass River catchment, New South Wales, Australia. Hydrogeol J 5:71–88

Kortatsi BK, Tay CK, Anornu G, Hayford E, Dartey GA (2008) Hydrogeochemical evaluation of groundwater in the lower Offin basin, Ghana. Environ Geol 53(8):1651–1662

Kumar M, Ramanathan AL, Rao MS, Kumar B (2006) Identification and evaluation of hydrogeochemical processes in the groundwater movement of Delhi, India. Environ Geol 50(7):1025–1039

Legchenko A, Descloitres M, Bost A, Ruiz L, Reddy M, Girard JP, Sekhar M, Mohan Kumar MS, Braun J-J (2006) Resolution of MRS applied to the characterization of hard—rock aquifers. Groundwater 44:547–554

Li X, Zhand L, Hou X (2008) Use of hydrogeochemistry and environmental isotopes for evaluation of groundwater in Qingshuihe basin, northwestern China. Hydrogeol J 16(2):335–348

Maréchal J-C, Dewandel B, Ahmed S, Galeazzi L, Zaidi FK (2006) Combined estimation of specific yield and natural recharge in a semi-arid groundwater basin with irrigated agriculture. J Hydrol 329(1–2):281–293

Maréchal J-C, Murari RRV, Riotte J, Vouillamoz JM, Mohan Kumar MS, Ruiz L, Sekhar M, Braun J-J (2009) Indirect and direct recharge in a tropical forested watershed: Mule Hole, India. J Hydrol 364(3–4):272–284

Martin C, Aquilina L, Gascuel-Odoux C, Molenat J, Faucheux M, Ruiz L (2004) Seasonal and interannual variations of nitrate and chloride in stream waters related to spatial and temporal patterns of groundwater concentrations in agricultural catchments. Hydrol Process 18(7):1237–1254

Négrel Ph, Lemiére B, Machard de Grammont H, Billaud B, Sengupta B (2007) Hydrogeochemical processes, mixing and isotope tracing in hard rock aquifers and surface waters from the Subarnarekha river basin (east Singhbhum district, Jharkhand state, India). Hydrogeol J 15(8):1535–1552

Négrel Ph, Pauwels H, Dewandel B, Gandolfi JM, Mascre C, Ahmed S (2011) Understanding of groundwater systems and their functioning through the study of stable isotopes in a hard-rock aquifer (Maheshwaram watershed, India). J Hydrol 397(1–2):55–70

Pacheco F, Van der Weijden CH (1996) Contributions of water–rock interactions to the composition of groundwaters in areas with a sizeable anthropogenic input: a case study of the water of the Fundao area, central Portugal. Water Resour Res 32(12):3553–3570

Pasi P, Mats A (2008) Urban geochemistry: a multimedia and multielement survey of a small town in northern Europe. Environ Geochem Health 25(4):397–419

Perrin J, Ahmed S, Hunkeler D (2011) The effects of geological heterogeneities and piezometric fluctuations on groundwater flow and chemistry in a hard rock aquifer, southern India. Hydrogeol J 19(6):1189–1201

Piper AM (1944) A graphic procedure in the geochemical interpretation of water analyses. Am Geophys Union Trans 25:914–923

Purushotham D, Prakash MR, Narsing Rao A (2011) Groundwater depletion and quality deterioration due to environmental impacts in Maheshwaram watershed of R.R. district AP (India). Environ Earth Sci 62(8):1707–1721

Rajasekharan G (2003) District handbooks of Kerala, Wayanad, vol 1. Dep of Inf and Public Relat, pp 4–10

Rajesh R, Brindha K, Murugan R, Elango L (2012) Influence of hydrogeochemical processes on temporal changes in groundwater quality in a part of Nalgonda district, Andhra Pradesh, India. Environ Earth Sci 65(4):1203–1213

Rajmohan N, Elango L (2006) Hydrogeochemistry and its relation to groundwater level fluctuation in the Palar and Cheyyar river basins, southern India. Hydrol Process 20(11):2415–2427

Ramos-Leal JA, Martinez-Ruiz VJ, Rangel-Mendez JR, Alfaro de la Torre MC (2007) Hydrogeological and mixing process of waters in aquifers in arid regions: a case study in San Luis Potosi valley, Mexico. Environ Geol 53(2):325–337

Rao NS, Rao PS (2010) Major ion chemistry in a river basin: a study from India. Environ Earth Sci 61(4):757–775

Rasmussen P (1996) Monitoring shallow groundwater quality in agricultural watersheds in Denmark. Environ Geol 27(4): 309–319

Reddy DV, Nagabhushanam P, Sukhija BS, Reddy AGS (2009) Understanding hydrological processes in a highly stresses granitic aquifer in southern India. Hydrol Process 23(9):1282–1294

Ruiz L, Varma MRR, Mohan Kumar MS, Sekhar M, Maréchal J-C, Descloitres M, Riotte J-J, Kumar Sat, Kumar C, Braun J-J (2010) Water balance modeling in a tropical watershed under deciduous forest (Mule Hole, India): Regolith matric storage buffers the groundwater recharge process. J Hydrol 380(3–4):460–472

Ryu J-S, Lee K-S, Chang H-W, Shin HS (2008) Chemical weathering of carbonates and silicates in the Han river basin, South Korea. Chem Geol 247(1–2):66–80

Sekhar M, Rasmi SN, Sivapullaiah PV, Ruiz R (2004) Groundwater flow modeling in Kabini river basin, India. Asian J Water 1(2–4):65–77

Sharma A, Singh AK, Kumar K (2012) Environmental geochemistry and quality assessment of surface and subsurface water of Mahi River basin, western India. Environ Earth Sci 65(4):1231–1250

Shi JA, Wang Q, Chen GJ, Wang GY, Zhang ZN (2001) Isotopic geochemistry of the groundwater system in arid and semi-arid areas and its significance: a case study in Shiyang river basin, Gansu province, northwest China. Environ Geol 40(4–5): 557–559

Singh AK, Mondal GC, Kumar S, Singh TB, Tewary BK, Singh A (2008) Major ion chemistry, weathering processes and water quality assessment in upper catchment of Damodar river basin, India. Environ Geol 54(4):745–758

Song X, Kayane I, Tanaka T, Shimada J (1999) Conceptual model of the evolution of groundwater quality at the wet zone in Sri Lanka. Environ Geol 39(2):149–164

Soumya BS, Sekhar M, Riotte J-J, Braun J-J (2008) Hydrochemistry in the narrow zone of climatic variation in the Kabini river basin, Southern India. In: Water down under 2008—Proceedings of the International Conference at Adelaide, Australia

Soumya BS, Sekhar M, Riotte J-J, Braun J-J (2009) Non-linear regression model for spatial variation in precipitation chemistry for South India. Atmos Environ 43(5):1147–1152

Soumya BS, Sekhar M, Riotte J-J, Audry S, Lagane C, Braun J-J (2011) Inverse models to analyze the spatiotemporal variations of chemical weathering fluxes in a granito-gneissic watershed: Mule Hole, South India. Geoderma 165(1):12–24

Sreedevi PD, Ahmed S, Made B, Ledoux E, Gandolfi JM (2006) Association of hydrogeological factors in temporal variations of fluoride concentration in a crystalline aquifer in India. Environ Geol 50(1):1–11

Stigter TY, Van Ooijen SPJ, Post VEA, Appelo CAJ, Dill MMC (1998) A hydrogeological and hydrochemical explanation of the groundwater composition under irrigated land in a Mediterranean environment, Algarve, Portugal. J Hydrol 208(3–4): 262–279

Sukhija BS, Reddy DV, Nagabhushanam P, Bhattacharya SK, Jani RA, Kumar D (2006) Characterization of recharge processes and groundwater flow mechanisms in weathered—fractured granites of Hyderabad (India) using isotopes. Hydrogeol J 14:663–674

Tripathi JK, Rajamani V (2007) Geochemistry and origin of ferruginous nodules in weathered granodioritic gneisses, Mysore Plateau, Southern India. Geochim Cosmochim Acta 71:1674–1688

Tsujimura M, Abe Y, Tanaka T, Shimada J, Higuchi S, Yamanaka T, Davaa G, Oyunbaatar D (2007) Stable isotopic and geochemical characteristics of groundwater in Kherlen River basin, a semi-arid region in eastern Mongolia. J Hydrol 333:47–57

Umar R, Ahmed I, Alam F, Khan MM (2009) Hydrochemical characteristics and seasonal variations in groundwater quality of an alluvial aquifer in parts of Central Ganga Plain, Western Uttar Pradesh, India. Environ Geol 58(6):1295–1300

Vijith H, Satheesh R (2007) Geographical Information System based assessment of spatiotemporal characteristics of groundwater quality of upland sub-watersheds of Meenachil river, parts of Western Ghats, Kottayam district, Kerala, India. Environ Geol 53(1):1–9

Violette A, Riotte J-J, Braun J-J, Oliva P, Maréchal J-C, Sekhar M, Jeandel C, Subramanian S, Prunier J, Barbiero L, Dupre B (2010) Formation and preservation of pedogenic carbonates in South India, links with paleomonsoon and pedological conditions: clues from Sr isotopes, UTh series and REEs. Geochim Cosmochim Acta 74(24):7059–7085

WHO (1997) Guidelines for drinking water-quality, vol 1, recommendations. World Health Organisation, Geneva

Wilcox LV (1955) Classification and use of irrigation waters. US Department of Agriculture, Cir 969, Washington DC

Zhu GF, Su YH, Feng Q (2008) The hydrochemical characteristics and evolution of groundwater and surface water in the Heihe river basin, northwest China. Hydrogeol J 16(1):167–182